Data User Guide

Deliverable title	Data User Guide
Deliverable number	D4.2
Revision	00
Status	Final
Planned delivery date	30/04/2013
Date of issue	08/05/2013
Nature of deliverable	Report
Lead partner	BIRA-IASB
Dissemination level	Public

This work has received research funding from the European Community's Seventh Framework Programme ([FP7/2007-2013]) under grant agreement n°284421.

SEVENTH FRAMEWORK PROGRAMME

DOCUMENT PROPERTIES

	FUNCTION	NAME	ORGANISATION	DATE	SIGNATURE
LEAD AUTHOR	Research Associate	M. De Mazière	BIRA-IASB	5/5/2013	
CONTRIBUTING AUTHORS	Research Associate	A. Richter	Univ. Bremen		
	Research Associate	M. Pastel	LATMOS/CNRS		
	Research Associate	F. Hendrick	BIRA-IASB		
	Research Associate	B. Langerock	BIRA-IASB		
	Research Associate	K. Hocke	IAP/U. Bern		

Table of Contents

Executive summary

Contents

List of tables

List of figures

EXECUTIVE SUMMARY

CONTENTS

I. Fourier-transform Infrared Spectrometry (FTIR)

A. Instrument fiche

Table 1. FTIR Instrument fiche. Adapted from [ISSI, 2012, Annex A.1.3].

Instrument	Fourier transform infrared spectrometer (Michelson-type interferometer)
Platform	ground-based
Measuring technique	Solar (or lunar) absorption spectrometry
Observation geometry	Looking directly at the center of the sun (or the moon)
Units	Total columns (mol/cm2) and volume mixing ratio per atmospheric layer (vmr) and partial column per atmospheric layer (mol/cm2)
Vertical resolution	A few km to 10 km
Horizontal resolution	Depending on solar zenith angle of measurement and vertical profile of the target species: the horizontal resolution decreases as the SZA increases and if the target gas is located higher in the atmosphere.
Temporal resolution	Depending on the spectral resolution and number of interferometer scans per spectrum (the higher the spectral resolution and the number of scans per spectrum, the worse the temporal resolution)
Vertical range	0-70 km
Horizontal range	about 5x5km at 50 km
Stability/drift	avoided by instrument line shape verifications with a known cell measurement (typically HBr or N2O)
Precision	
Systematic uncertainty	Mainly determined by spectroscopic uncertainties (5 – 20%)
Daytime/ nighttime	Only daytime for solar absorption; nighttime data with lunar absorption are generally less precise
Weather conditions	Stable optical depth is required in FOV; essentially clear sky is required
Interferences/ contamination (payload, spectral)	Minor contaminations due to spectroscopic interferences with other species, like H2O, CH4, …. In general they are minimized.
Bottlenecks, limitations	Large, heavy and expensive instrument; limited or no transportability; open view to the sun is required all day; air-conditioned room is required. The instrument must be operated with a

	reliable suntracking system.
Absolute or calibration needed?	Self-calibrating technique (differential absorption principle)
Corrections needed?	No
Auxiliary data	Pressure / Temperature profiles from local observations or NCEP.
Averaging kernels	Important component of the retrieval products (L2): give information about sensitivity of the data products to the true and the a priori profiles.
A priori information	A priori information on atmospheric vertical profiles for target and interfering species is required in the L1-> L2 retrieval process; taken from WACCM output; sometimes adjusted via a dedicated pre-fit of observed spectra.
Spectroscopic parameters	from spectroscopic databases (HITRAN or pseudolines from JPL (G. Toon) or specific databases)
Transportability/ Suitability for campaign	Bruker 120/125 M is transportable and therefore suitable for campaigns; Bruker 120/125 HR are not transportable unless if installed in a transportable container.
System availability	Commercial spectrometers
Data processing time	The goal is to deliver L2 data within 1 month after spectra acquisition
Additional products	Interfering species concentrations, in particular H_2O
Future potential	Delivery of more species, more information about isotopologues for some species (H_2O, CO, CH_4,…); delivery of horizontal averaging kernels ?
Caveats	Averaging kernels (vertical and horizontal) and a priori information required for proper interpretation of the L2 data.

B. Operation mode

Figure 1. Experimental set-up

Figure 1 shows an experimental setup. Top left: meteostation; top right: suntracker; bottom: Fourier transform spectrometer. The meteo station includes a Vaisala wind/humidity/rain detector (in the red circle), a sunshine detector (total solar irradiance) (in the green circle), a high-precision barometer (in the orange circle) and a presence-of-rain detector (in the yellow circle).

The solar (lunar) light is guided into the spectrometer by a precise suntracker that follows the sun during the day. The system has an active feedback system, in order to keep the sun image at all times centered on the entrance aperture of the spectrometer. The alignment of the solar beam in the spectrometer is critical, and is verified regularly with a cell measurement: the measurement with high-spectral resolution (of order 0.003 cm-1) of the absorption spectrum of a known gas (e.g., HBr, N_2O, CS_2) with a known concentration at low pressure in the cell reveals the instrument line shape and permits verification of the alignment.

The spectrometer is equipped with an InSb detector covering the range 1 to 5 µm, and a HgCdTe detector covering the range 1.5 to 16 µm. Both detectors are cooled to liquid N_2 temperatures.

The recorded signal (L0) is an interferogram, which is then transformed via a Fast Fourier Transform (FFT) algorithm into a spectrum (L1 data) (Figure 2). In order to increase the signal-to-noise ratio, an optical filter in front of the detector limits the spectral bandwidth of the recorded spectra. The interferogram corresponds to the AC part of the detector signal; ideally the DC part is also recorded to verify the signal strength.

For operational measurements the ground-based FTIR spectra are measured with a typical resolution of about 0.005 cm^{-1} (i.e. maximum optical path difference, OPD, of 180 cm), which corresponds to a resolution $\lambda/\delta\lambda$ at 1000 cm^{-1} of approx. 2×10^5.

To increase even more the signal-to-noise ratio, several interferometer scans may be co-added before transformation into a spectrum.

Recording of one spectrum requires between one to a few tens of minutes, depending on the required spectral resolution and signal-to-noise ratio. During the whole recording time, the solar (lunar) intensity (in the infrared) must be stable. This can be guaranteed only with completely clear sky.

In many instances, and especially in remote locations, the experiment is performed in automatic or remote control mode. This requires knowledge about the meteorological conditions, via a small meteorological station. Most important meteo parameters are the presence of rain, in which case the suntracker must be closed, the solar irradiance, to verify the solar intensity, and the local surface pressure and temperature. Additional parameters are wind speed and direction, and local humidity. The meteorological data are stored at a high frequency (of order 1s).

In some cases, the spectral radiances are calibrated against a blackbody – see [ISSI, 2012].

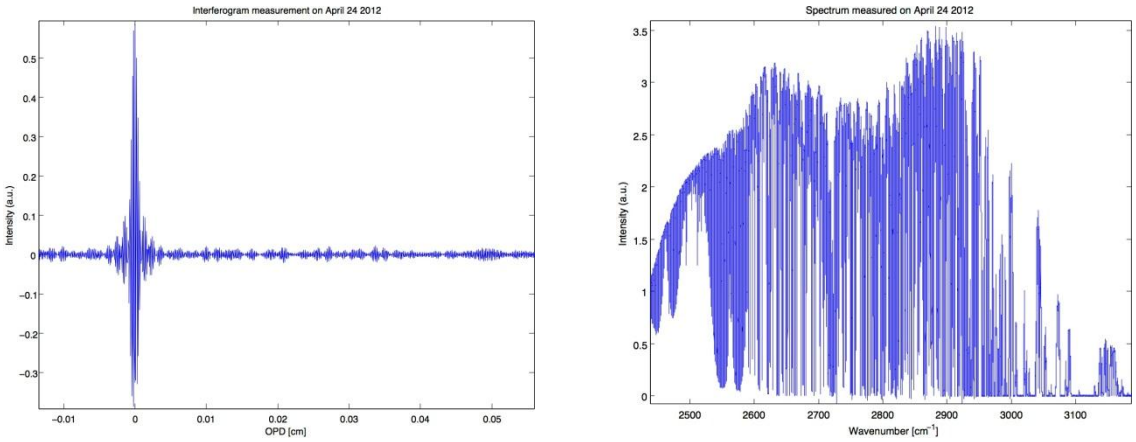

Figure 2. Example of an interferogram and associated spectrum, in the spectral range 2450-3200 cm-1, recorded on April 24, 2012 at St. Denis, Ile de La Réunion (21°S, 55°E, approximately sea level).

C. L1 data

As explained above, the L1 data are spectra, covering a given spectral bandwidth. Some preprocessing is performed before they are ingested in the inversion to derive the L2 products.

The preprocessing essentially includes re-formatting, calculation of the solar zenith and azimuth angle characterizing the spectrum, synchronization between the spectra and the meteorological data, and rejection of bad spectra, based on the meteorological parameters and the detector DC signal.

D. L1 →L2 data processing principles

The observed spectra (I as a function of wavenumber ν) are representative of the absorption of the solar beam along the line of sight (s) in the atmosphere. In other words, they provide integrated information along the line of sight, which is completely determined by the geographical location of the spectrometer, and the solar (lunar) zenith and azimuth angles associated with the spectrum. The latter parameters are all included in the data files. Figure 3 provides an example of a spectrum in the window 1002-1003 cm^{-1} in which several ozone absorption lines are present.

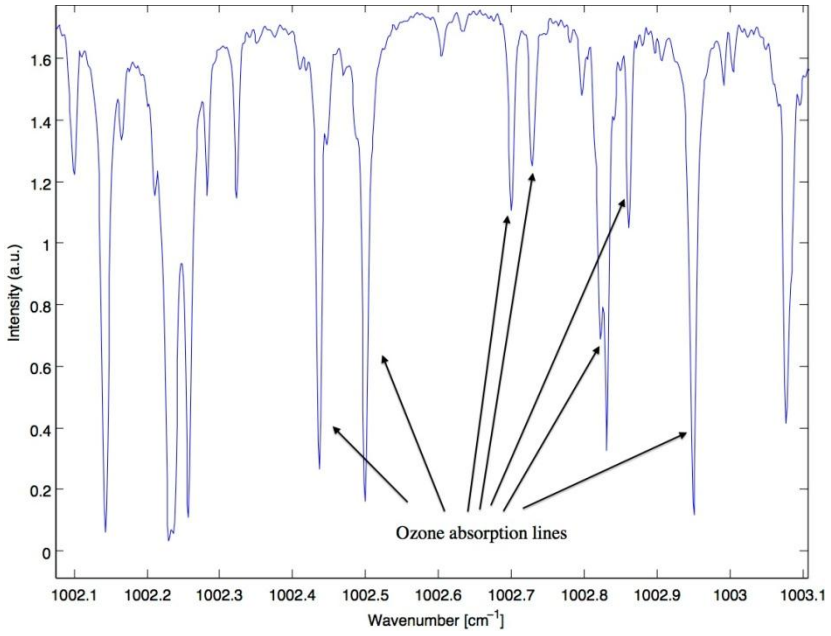

Figure 3. Example of the spectral microwindow 1002-1003 cm^{-1} which contains several ozone absorption lines, from a spectrum taken at St Denis, Ile de La Réunion.

The retrieval process or inversion (L1→ L2) consists of extracting from the spectra the information about the absorbers' concentrations and vertical distributions in the atmosphere, based on the basic radiative transfer equations (Schwarzwild's equation):

$$dI_{\upsilon}(s_0, \vec{s}) = -\alpha_{ext} I_{\upsilon}(\vec{s}) ds + \alpha_{ext} J_{\upsilon}(\vec{s}) ds = -\alpha_{ext} (I_{\upsilon}(\vec{s}) - J_{\upsilon}(\vec{s})) ds \quad (1)$$

In the solar absorption case, the only source term (J) to be considered is the sun, and in the infrared, one can omit scattering and therefore, the extinction coefficient (α_{ext}) reduces to the absorption coefficient (α_{abs}). The equation can be re-written as:

$$I(\nu)/I_{sun}(\nu) = \exp(-\int_{\infty}^{s_0} \alpha_{abs}\left(\nu, s(P,T)\right)x(s)ds) \qquad (2)$$

in which x(s) is the absorber's concentration at position s along the line of sight. The equation is written in the case of one single absorber; in practice of course, the extinction factors due to every single absorber must be multiplied.

The 'inversion' of this equation enables therefore the determination of the absorbers' concentrations, assuming perfect knowledge of the light path trajectory and of the absorption coefficients and their dependence on P and T.

In practice, the solution of the equation is not unequivocal (ill-posed problem) and some a priori knowledge must be used to find the most probable solution. The methods most often used at present are the Optimal Estimation Method and Tikhonov regularization [Rodgers, 2000]. The mathematics are shortly summarized in [ISSI, 2012].

The inversion then yields the retrieved vertical distribution x_r along the vertical *(z)* of the target absorber(s) in the atmosphere:

$$x_r(z) = x_a + A(x_t - x_a) \qquad (3)$$

in which x_a *and* x_t are the a priori and true vertical profiles of the target absorber, respectively, and A is a product of the retrieval process, the so-called Averaging Kernel (a square matrix).

E. L2 data and use caveats

The L2 data consist of the retrieved vertical profiles $x_r(z)$, expressed as a volume mixing ratio (VMR) on a vertical altitude grid.

In addition, the data files also provide the integrated profiles or total columns and the partial columns per altitude layer defined by the layer altitude boundaries. With each variable, the associated random, systematic and total uncertainty is provided – see Guide to Data Uncertainties.

Since water vapour is an important interfering gas in the infrared, and since it is important to distinguish between the dry air VMR and the wet air VMR, the concentration profiles of H_2O are also provided in the data files.

One must be careful as to whether the VMR is specified as an effective mean VMR in the corresponding altitude layer, defined by the altitude boundaries, or as a VMR on one of the layer boundaries: this is explained in the variable descriptions associated with the ALTITUDE, ALTITUDE.BOUNDARIES, MIXING.RATIO and COLUMN.PARTIAL variables in the data files.

One must be well aware about the interpretation of the retrieved vertical profiles:

The above equation (3) tells you how the retrieved profile is related to the true profile and what the contribution is of the a priori in the retrieved profile. An averaging kernel close to the identity matrix tells you that the retrieval is close to the truth and the a priori contribution is very small. An averaging

kernel close to zero tells you that you're almost reproducing the a priori, in other words, the measurements have not added a lot of information.

The averaging kernel also provides you the information about the vertical resolution: the vertical resolution cannot be expressed as a single number; rather it is described by the convolution of the true profile with the averaging kernel.

Both x_a and A are provided in the data files.

A determines the so-called smoothing error of the retrieval products, as described in the Guide to Data Uncertainties.

F. Including concept/examples of horizontal/vertical averaging

Vertical averaging

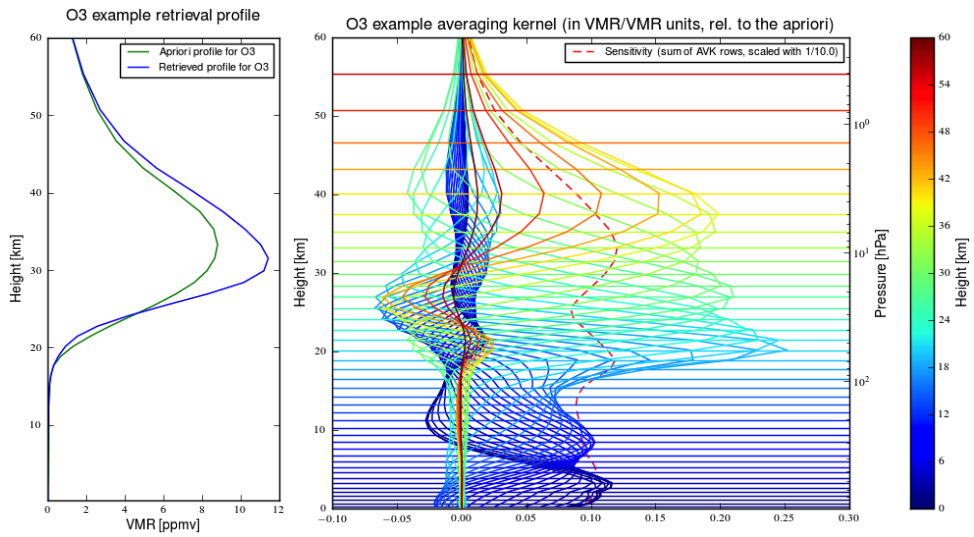

Figure 4. Example of ozone retrieval (left plot: green profile is the a priori; blue profile is the retrieved one) and associated averaging kernel in VMR/VMR units (right plot). The dashed curve in the latter plot represents the sensitivity curve (see text).

The above picture presents a typical averaging kernel (AVK) matrix for an O_3.retrieval. The AVK matrix is defined on the same vertical grid as the retrieved profile. The colored curves in the plot are the rows of the AVK matrix where each element in a row is plotted against the corresponding height grid. Each curve or row of the AVK is color coded according to the height of the corresponding row index (see horizontal lines). The sensitivity curve represents the fractional sensitivity of the retrieved profile at each altitude to the measurement.

The AVK matrix determines how the retrieved profile is related to the true and the a priori profiles, according to Eq. (3). For example, the retrieved profile at 40 km altitude is obtained from Eq. (3) with the row of AVK corresponding to 40km, i.e., the yellow curve in the AVK plot in Figure 4. The yellow curve has a peak at 40km, but has non vanishing terms on the nearby altitude layers.

Ideally each row has a single discrete peak at its corresponding height, but in OEM the retrieved information at a certain altitude is obtained also from nearby layers. And at higher altitudes there is no

information at all (the red lines tend to zero). There the retrieved profile reproduces the a priori vertical profile.

Comparing FTIR retrieved profiles with other 'reference' data (e.g. model, satellite) requires that these reference data undergo the same 'averaging' of information as a function of altitude (i.e., convolution with the averaging kernel) in order to obtain comparable objects. E.g., one does not wish to obtain an apparent bias at altitudes where the measurement has no sensitivity. This averaging or smoothing of the reference data is essentially Equation (3), where x_t is replaced by the reference data.

Horizontal averaging

The retrieved profiles are not measured exactly at the instruments location: depending on the solar zenith and azimuth angles, the line of sight differs. A horizontal averaging kernel of a measurement describes the relationship between the information in the retrieved profile and its geographical location. These horizontal averaging kernels are not available in the HDF data files and FTIR data users should realize that the data is not geographically located at the instruments location. The users can estimate the geographical location of the information from the solar and azimuth angles that are provided in the HDF files and a ray-tracing tool.

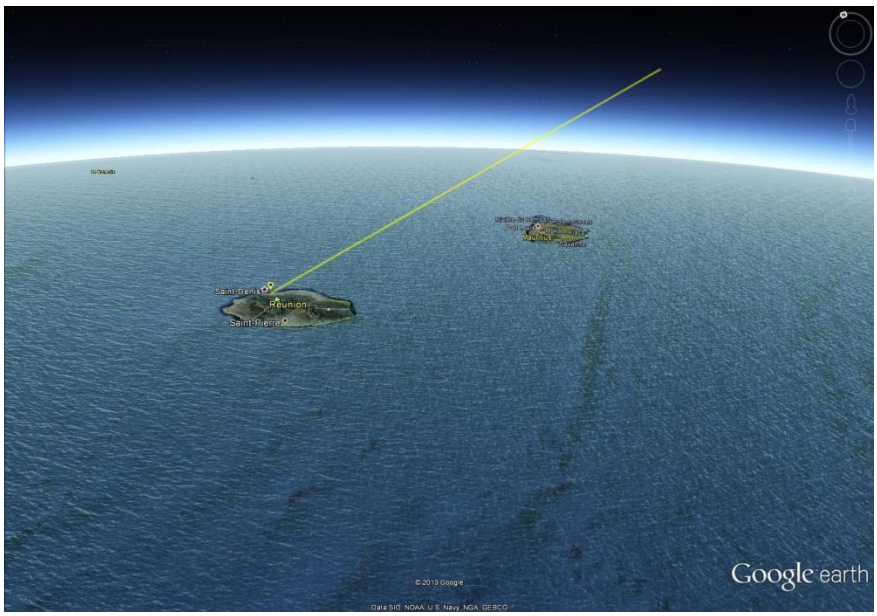

Figure 5. Example of the light path for a measurement at St Denis Ile de La Réunion with a high solar zenith angle.

Table 2. Example of a ray tracing output for an FTIR measurement of CH4 at St Denis (-20.9°S, 55.5°E), Ile de La Réunion, on 25/1/2011 04:04 UT for a solar zenith angle of 62° and an azimuth angle of 101° measured from N (0°) to E (90°). The Table provides the geographical location of the points along the line of sight corresponding to a percentage of the total CH_4 column.

Percentage	Latitude (° North)	Longitude (° East)	Altitude (km)	Distance from instrument location (km)
0	-20.900	55.480	0.05	0.0
20	-20.906	55.511	1.8	3.3
40	-20.912	55.546	3.8	7.0
60	-20.921	55.596	6.6	12.3
80	-20.934	55.666	10.6	19.7

Table 3. Example of a ray tracing output for O3 providing the geographical location of the points along the line of sight corresponding to a percentage of the total O3 column (measurement on 25/1/2011 4:04 UT with solar zenith angle 62° and azimuth angle 101° (measured from N (0°) to E(90°))

Percentage	Latitude North (°)	Longitude East (°)	Altitude (km)	Distance from instrument location (km)
0	-20.900	55.480	0.1	0.0
20	-20.947	55.740	14.8	27.5
40	-20.963	55.827	19.8	36.8
60	-20.975	55.893	23.6	43.8
80	-20.991	55.980	28.6	53.0

G. References

ISSI, 2012: Schneider, Matthias, Philippe Demoulin, Ralf Sussmann, and Justus Notholt, Fourier Transform Infrared Spectrometry, Chapter 6 *in Monitoring Atmospheric Water Vapour*, *Ground-Based Remote Sensing and In-situ Methods*, ISSI Scientific Report Series, Vol. No. 10 (Editor Niklaus Kämpfer), Springer, DOI 10.1007/978-1-4614-3909-7, 2012, ISBN 978-1-4614-3908-0, 2013.

Rodgers, C. D., Inverse methods for atmospheric sounding, Series on Oceanic and planetary physics – vol. 2, World Scientific, 2000.

II. DOAS / MAXDOAS

A. Instrument fiche

Table 4. DOAS/MAXDOAS instrument fiche

Instrument	Multi-AXis Differential Optical Absorption Spectrometer (MAX-DOAS)
Platform	ground-based
Measuring technique	Solar light absorption spectrometry
Observation geometry	Looking at scattered light from the zenith and various directions above the horizon. Some instruments also perform direct sun observations.
Units	Total columns (mol/cm2) and volume mixing ratio per atmospheric layer (vmr) and partial column per atmospheric layer (mol/cm2)
Vertical resolution	Strongly varying from 100 m close to the ground to column above 5 km
Horizontal resolution	Depending on solar zenith angle of measurement, vertical layer position and wavelength range used and atmospheric aerosol load and vertical profile of the target species: the horizontal resolution decreases as the SZA increases and if the target gas is located higher in the atmosphere. In the boundary layer, it decreases with increasing aerosol load and towards shorter retrieval wavelengths.
Temporal resolution	Better than 1 minute for tropospheric column, 10 minutes for stratospheric columns at twilight, typically 15 – 30 minutes for profile in the troposphere
Vertical range	0-70 km
Horizontal range	0 – 50 km in the troposphere
Stability/drift	avoided by thermal stabilisation, use of zenith reference spectra and instrument line shape verifications with spectral measurements and / or numerical determination of slit width
Precision	???
Systematic uncertainty	Determined by spectroscopic uncertainties (5 – 10%) and radiative transfer uncertainties (10 – 20%)
Daytime/ nighttime	Only daytime
Weather conditions	Best measurements at clear sky, good tropospheric profiles at homogeneous cloud conditions, stratospheric columns nearly independent of weather conditions. Direct sun observations only possible if solar disk is visible.
Interferences/ contamination	Spectral interferences for weak absorbers at low concentrations possible

(payload, spectral)	
Bottlenecks, limitations	Relatively sensitive instrument, air-conditioned room is required for many research grade instruments, tracker used. High aerosol load and broken clouds limits accuracy and resolution of tropospheric profiles
Absolute or calibration needed?	Self-calibrating technique (differential absorption principle)
Corrections needed?	No
Auxiliary data	No
Averaging kernels	Important component of the retrieval products (L2): give information about sensitivity of the data products to the true and the a priori profiles.
A priori information	A priori information on atmospheric vertical profiles for target and their covariances are needed in Optimal Estimation type profile retrievals.
Spectroscopic parameters	from spectroscopic databases
Transportability/ Suitability for campaign	Depending on instrument type: Mini-DOAS (excellent) to scientific grade instruments (suitable but container or air conditioned room needed)
System availability	Commercial spectrometers, for scientific grade instruments with custom built telescopes, thermal stabilisation and calibration units.
Data processing time	The goal is to deliver L2 data within 1 month after spectra acquisition
Additional products	
Future potential	
Caveats	Averaging kernels (vertical and horizontal) and a priori information required for proper interpretation of the L2 data.

B. Operation mode

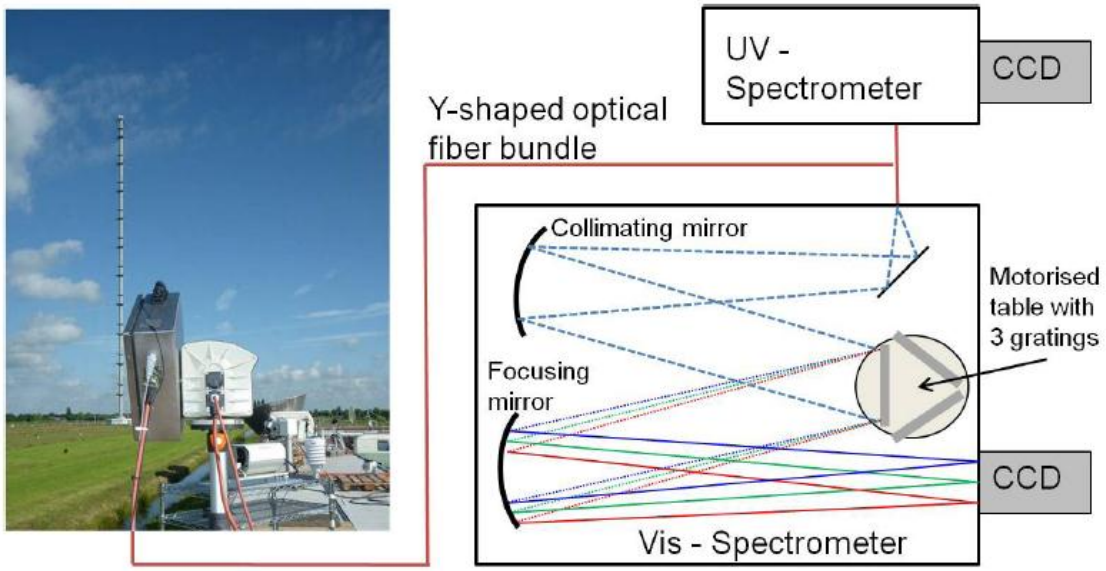

Figure 6. Experimental setup

Figure 6 shows an experimental setup. Instruments usually consist of a pointable telescope, connected to a spectrometer via quartz fibre bundle and connected to a temperature stabilised grating spectrometer equipped with a CCD detector. Miniaturized systems exist that integrate all components into one box. The example shown is for the IUP-UB instrument used during the CINDI intercomparison campaign; it has two channels, one for the UV and one for the visible part of the spectrum.

In a Multi-AXis or MAX-DOAS instrument, light is guided into the spectrometer by a telescope that can be pointed at the sun or at different parts of the sky. Depending on the instrument and application, different operation modes can be used:

1. Zenith sky operation for total columns, stratospheric profiles and tropospheric columns with low sensitivity
2. Direct sun operation for total columns and in combination with scattered light observations for atmospheric profiles
3. Multi-Axis operation with multiple viewing directions above the horizon for tropospheric profiles and (if azimuthal pointing is possible) horizontal gradients.

Depending on application, one or several spectrometers are connected to the telescope via quartz fibre optics covering parts of the spectral range from 320 – 600 nm with spectral resolution of typically 0.2 – 1 nm. The spectrometers are usually equipped with cooled CCD detectors. Spectral filters are used to reduce straylight from wavelengths outside the spectral region of interest.

Exposure times depend on instrument type and illumination conditions and vary from milliseconds to seconds. To increase the signal-to-noise ratio, several measurements are averaged, typically over (several) minutes.

In MAX-DOAS applications, a series of measurements is taken at different elevation angles, typical values being 1°, 2°, 3°, 4°, 5°, 6°, 7°, 8°, 9°, 10°, 15°, 30°, 90° elevation. Additional viewing direction at different azimuths can be taken for horizontal gradients. A compromise has to be taken between minimising atmospheric changes between measurements (short measurements) and high signal to noise for the individual observations (longer measurements).

Instruments are usually fully automated and programmed, providing data through internet access or direct download. Many instruments are also equipped by video cameras to facilitate data analysis with respect to viewing conditions and identification of disturbances. As part of the measurement programme, calibration measurements for characterisation of detector dark signal are taken either with a shutter or at night and some instruments also perform regular line lamp measurements for instrument line shape monitoring.

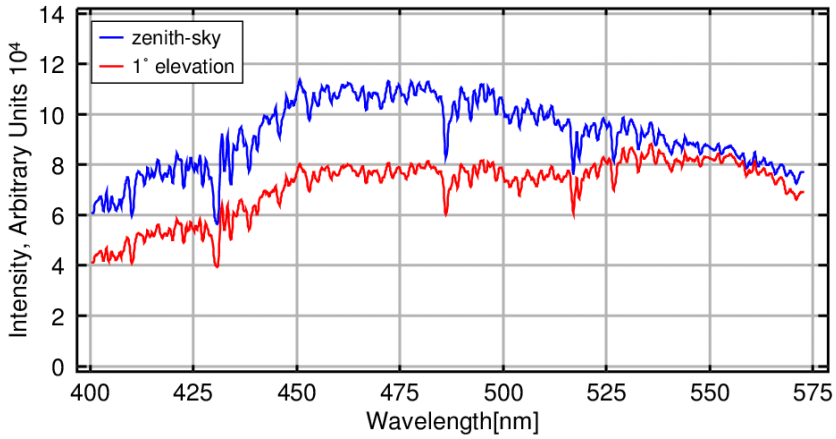

Figure 7. Example of two spectra taken during the CINDI campaign in Cabauw

Figure 7 is an example of two spectra (lv1) taken during the CINDI campaign in Cabauw, 51.96°N, 4.9°E on July 1st, 2009 around noon. The blue spectrum was taken in zenith direction while the red spectrum was measured at an elevation of 1° above the horizon. The spectra are dominated by Fraunhofer lines. The difference in slope is the result of scattering (zenith is bluer than the horizon).

C. L1 data

L1 data are spectra of intensity as a function of wavelength. Before use in the inversion, the dark signal of the detector is subtracted, data screening for too low (noisy) or too high (saturated) signals is performed, and a preliminary wavelength axis is assigned to the data. Additional information such as location, time of measurement, solar zenith and azimuth angle, the observation geometry and instrument settings is attached to the spectra.

D. L1 ->L2 data processing principles

Data analysis is divided into two steps:

1. Determination of atmospheric column amounts, integrated along the light path (slant column densities, SCDs) by application of the Differential Optical Absorption Spectroscopy method;
2. Conversion to vertical column densities (VCs) or vertical profiles

The DOAS fit is based on a linear least square solution of Lambert Beer's law for many wavelengths in parallel:

$$I(\lambda) = I_0(\lambda) \exp\left\{-\int \sigma(\lambda)\rho(s)ds\right\}$$

Here, I is the measurement spectrum and I_0 is a background spectrum, often a zenith-sky observation taken with the same instrument either at noon (for stratospheric retrievals) or very close in time to the current measurement (for tropospheric MAX-DOAS observations). A reference spectrum is needed to remove the effect of Fraunhofer lines which dominate the spectra recorded. The absorption cross-section σ is taken from spectroscopic data bases and the integral over the absorber density ρ along the light path is the slant column density SCD. In the atmosphere, several absorbers have to be taken into account as well as scattering. The effects of elastic scattering are accounted for as closure polynomials in wavelength; inelastic scattering is corrected using pseudoabsorbers derived from radiative transfer calculations:

$$\ln \frac{I_0(\lambda)}{I(\lambda)} = \sum_i \sigma_i(\lambda) SCD_i + \sum_p c_p \lambda^p$$

In order to improve the detection limit and the accuracy of the results, a non-linear component is included in the fit allowing spectral alignment between the two spectra used. For absolute wavelength calibration, alignment to a high resolution solar spectrum is performed, sometimes coupled to a fit of the instrument slit function.

The second step, retrieval of atmospheric vertical columns or profiles, can be performed in different ways, including

1. Conversion to vertical column densities by division of SCs by appropriate air mass factors, either from geometrical considerations or – more accurately – from radiative transfer calculations
2. Formal inversion of a series of measurements taken under different conditions (observation geometries for tropospheric columns and profiles, solar zenith angles for stratospheric columns and profiles) using Optimal Estimation in combination with a priori assumptions on the vertical profile of the substance of interest and its variability. The resulting lv2 product is the atmospheric profile together with its uncertainty and the averaging kernel.
3. Inversion of a series of measurements using a parameterised approach without a priori information. The resulting lv2 product are parameters characterising the atmospheric profile of the species (for example mixing height) and their uncertainties.

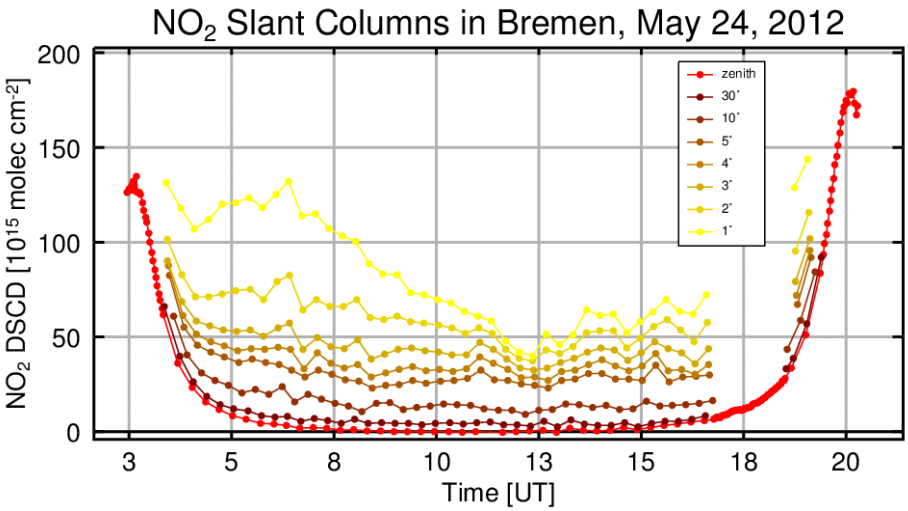

Figure 8. Example NO_2 differential slant columns (1v2a)

Figure 8 is an example of NO_2 differential slant columns (lv2a) measured in Bremen on May 24, 2012. All data are relative to the noon zenith observation; the gap around 18:00 UT is to avoid direct sunlight to enter the telescope. The larger columns in the lower elevation angles are indicative of strong pollution in the boundary layer.

E. L2 data and use caveats including concept/examples of horizontal/vertical averaging

Vertical averaging

When comparing MAX-DOAS trace gas and aerosol vertical profiles to correlative data (e.g., model, satellite, or FTIR), the difference in vertical resolution between both data sets must be taken into account. Since the MAX-DOAS profiles generally display the lowest vertical resolution, the correlative data should be degraded to the MAX-DOAS resolution in order to avoid apparent biases at altitudes where one measurement has no or little sensitivity. For an Optimal Estimation-based MAX-DOAS retrieval, this is done by convolving the correlative profiles with the coincident MAX-DOAS averaging kernels (AVK) using the following expression (Connor et al., 1994):

$$X_{c\_lr} = x_a + A\,(x_c - x_a)$$

where A is the MAX-DOAS averaging kernel matrix, x_a is the a priori profile used in the MAX-DOAS retrieval, x_c is the correlative high resolution profile, and x_{c_lr} is the smoothed or convolved correlative profile.

The averaging kernels, which are the rows of the A matrix, express the sensitivity of the retrieved profile with respect to the true atmospheric profile (Rodgers, 2000). Ideally, each averaging kernel should be a single discrete peak at its corresponding altitude. In practice, the information retrieved at a given altitude is also influenced by the nearby layers and hence, the averaging kernels are peaked functions with a half-width which is a measure of the vertical resolution. Typical MAX-DOAS averaging kernels for the NORS products (NO_2, HCHO, and aerosols) are shown in Figure 9.

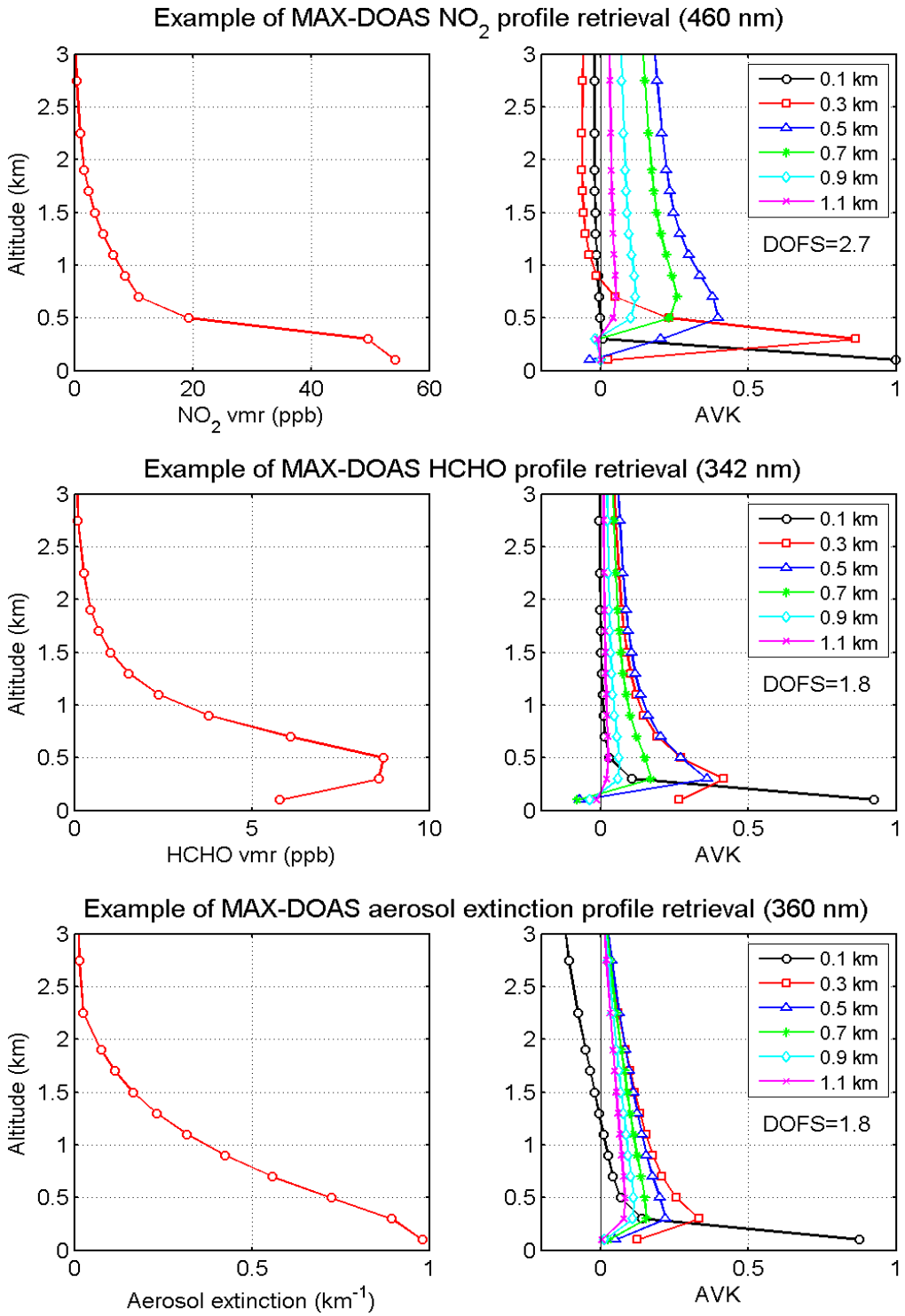

Figure 9. typical examples of MAX-DOAS profiles and averaging kernels for NO_2, HCHO, and aerosol retrievals.

Figure 9 shows typical examples of MAX-DOAS profiles and averaging kernels for NO_2, HCHO, and aerosol retrievals. Retrieved vertical profiles and corresponding averaging kernels are shown on the left and right plots, respectively. They have been obtained by applying the OEM-based bePRO profiling tool (Clémer et al., 2010) to MAX-DOAS observations at Xianghe, China, which is one of the candidate stations for the exportation of the NORS expertise (WP10). The aerosols retrieval is

performed from O_4 DSCDs at one wavelength only (intensities and other wavelength measurements not included). The number of independent pieces of information is given by the DOFS (degrees of freedom for signal).

The highest sensitivity is in the first layer (0-200m) for the three retrievals and the vertical resolution at this altitude is about 250m. At higher altitudes, the kernels quickly become broader and their peak values decrease, except for NO_2 which displays also a significant sensitivity in the 200-400m layer. It should be noted that for aerosols, the vertical resolution and information content can be increased by combining the O_4 differential slant column densities (DSCDs) and intensities at different wavelengths in the same retrieval (Frieß et al., 2006). These results show that the MAX-DOAS measurements are mostly sensitive to the layers close to the ground in addition to the tropospheric vertical column.

Twilight zenith-sky total ozone and stratospheric NO_2 vertical columns are also NORS products that should be delivered to the NORS/NDACC database. Within the NDACC UV-VIS Working Group, look-up tables of ozone and NO_2 column averaging kernels have been developed based on the Eskes and Boersma (2003) approach, i.e. the averaging kernel of a layer i can be approximated by the ratio of the box-air mass factor of this layer i and the total air-mass factor calculated from ozone and stratospheric NO_2 profile climatologies. More details on these averaging kernel tools can be found on the home page of the NDACC UV-VIS Working Group (*http://www.ndacc.org*). Figure 10 shows typical examples of ozone and NO_2 column averaging kernels calculated for 90°SZA (solar zenith angle) sunset at 45°N in April. The wavelengths are fixed to 475 nm (NO_2) and 510 nm (O_3).

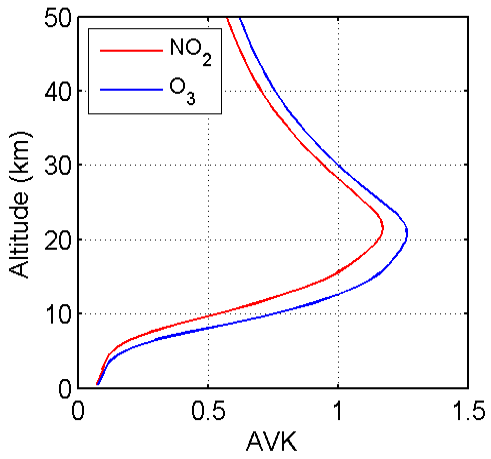

Figure 10. Typical examples of ozone and NO_2 column averaging kernels computed for 90° SZA sunset and 45°N in April.

The sensitivity of zenith-sky twilight measurements to the troposphere is limited, with averaging kernel values smaller than 0.5 below 8-10 km altitude. It increases in the stratosphere where averaging kernel values larger than 1 are obtained in the ~12-30 km altitude range, indicating that these measurements are strongly weighted by the contribution of the stratosphere.

MAX-DOAS and zenith-sky twilight averaging kernels will be included in the HDF data files delivered to the NORS/NDACC database.

Retrieval and Impact of Aerosols

The inversion of aerosol vertical profiles is based on measurements of the oxygen collision complex O_4 which shows pronounced absorption features around 360, 477, 577 and 630 nm. The retrieval of aerosol vertical profiles is based on the fact that the concentration of O_4 is proportional to the concentration of O_2. Therefore variations in O_4 can be related to changes in aerosol abundance. A simultaneous use of O_4 measurements at several wavelengths can significantly increase the information content. During clear-sky conditions, the intensity observed in off-axis geometry relative to the zenith measurement can be additionally used as input for the retrieval.

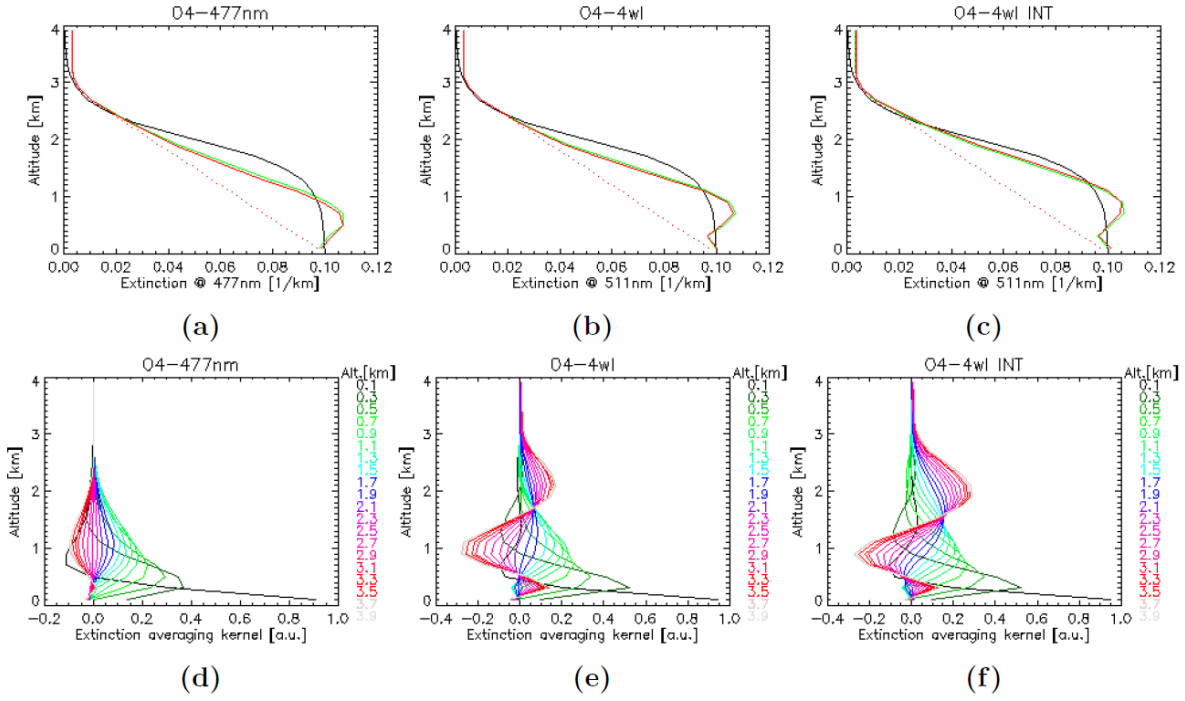

Figure 11. Example for retrievals (top) and averaging kernels (bottom) of the aerosol extinction profile based on synthetic measurements.

Figure 11 (a,d): Retrieval using only O_4 at 477 nm; (b,e): combined retrieval with O_4 at 360, 477, 577 and 630 nm; (c,f): combined retrieval with O_4 and relative intensity at 360, 477, 577 and 630 nm. The upper panels show the true (black), a priori (dotted red) and retrieved (solid red) profiles, as well as the true profile convolved with the averaging kernel (green).

Figure 12 shows retrieved aerosol extinction profiles, together with the corresponding averaging kernels, for retrievals using only a single O_4 absorption band, multiple O_4 absorption bands, as well as simultaneously multiple O_4 absorption bands and relative intensity. The colour code of the averaging kernels indicates the retrieval altitude. Each of these curves quantifies the sensitivity of the retrieved profile at given altitude to the true profile, providing a measure for the sensitivity and vertical resolution. In this example, the sensitivity of the retrieval is restricted to the lowermost 2 km of the atmosphere, but the sensitivity for the 2-3 km range improves significantly if several wavelengths and/or the relative intensity are considered in the retrieval. It is important to note that, owing to the non-linear nature of the inverse problem, the vertical resolution and information content of the aerosol retrieval strongly depend on the aerosol extinction profile

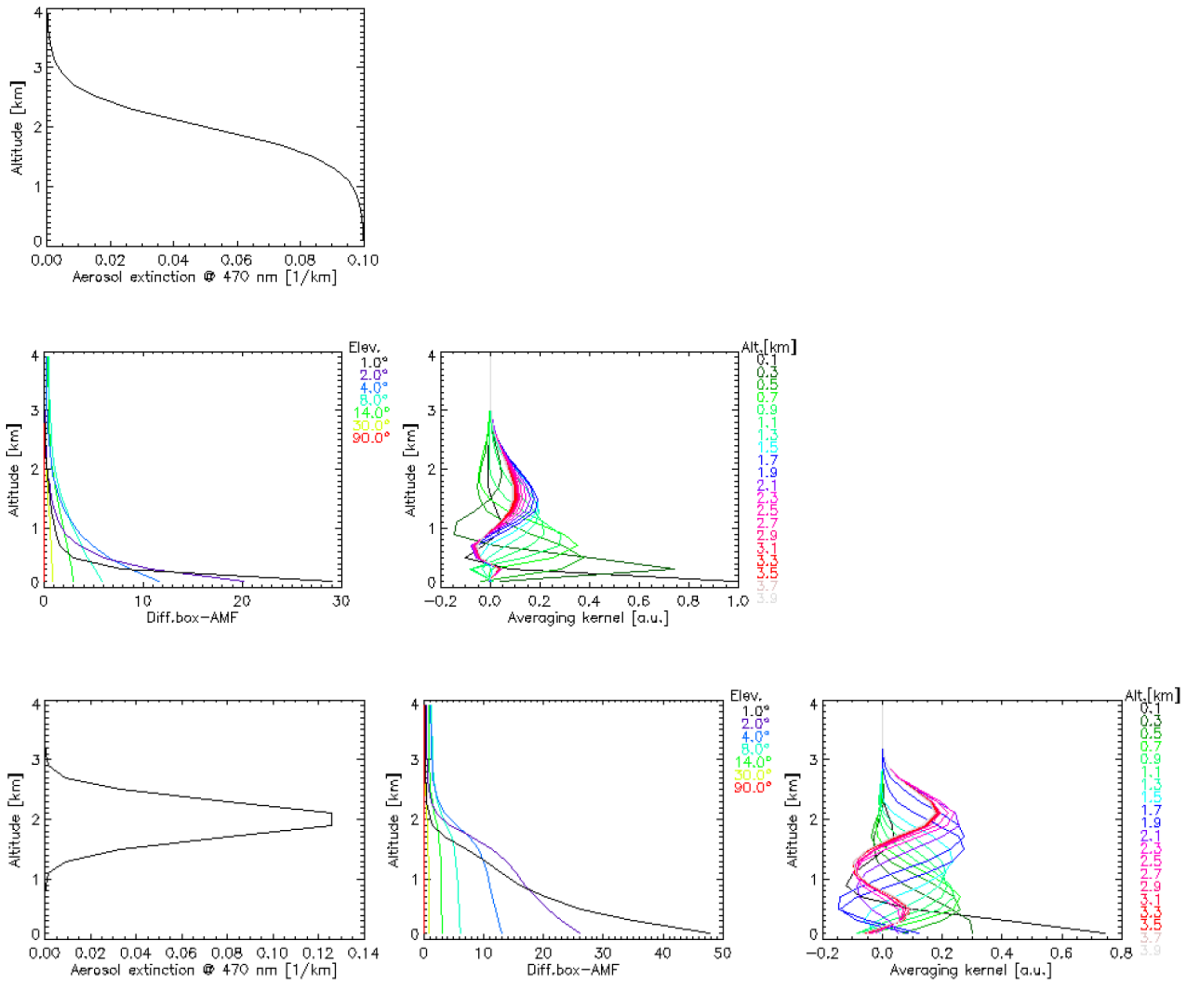

Figure 12. Example for the impact of the aerosol extinction profile on the NO2 retrieval. Left: Aerosol extinction profile; middle: NO2 Box-Airmass-Factors; right: NO2 averaging kernels.

The sensitivity of MAX-DOAS measurements on trace gases is significantly affected by the presence of aerosols and clouds.

In Figure 12, the top panels show a scenario with an aerosol layer from the surface up to 2 km, the bottom panels for an elevated aerosol profile centered around 2 km.This figure illustrates the impact of the aerosol vertical profile on the performance of the NO_2 vertical profile retrieval for an aerosol layer extending from the surface up to 2 km altitude as well as for an elevated aerosol layer centered around 2 km. It can be seen from the NO_2 Box-Airmass-Factor that an uplifted aerosol layer leads to an increase in light path at the altitudes where the aerosol is present. As indicated by the averaging kernels, an elevated aerosol layer results in an increase in sensitivity for NO_2 at higher altitudes, but a lower sensitivity right above the surface.

Horizontal averaging

The horizontal range, for which MAX-DOAS observations are sensitive, can be estimated from the measured O_4 absorption. The respective relationships between the retrieved O_4 DSCDs and the horizontal sensitivity ranges can be established based on radiative transfer simulations. Here we assume that the horizontal sensitivity range extends to the distance at which the O_4 DAMF (AMF at

low (e.g., 1°) elevation minus AMF at zenith) decreases to 1/e of its value at the location of the instrument (within 60 m distance).

The relationships between the retrieved O_4 DSCDs and the horizontal sensitivity ranges depend on wavelength, elevation angle and aerosol profile. Thus for the different wavelengths and elevation angles, separate relationships are determined (see below). In general, larger horizontal sensitivity ranges are found for vertically more extended aerosol extinction profiles. Further dependencies on SZA and relative azimuth angle are relatively small for SZA < 70° and will be ignored here.

In principle, especially at long wavelengths, the horizontal sensitivity range can become very large (>>100 km). However, such long distances are associated with air masses at rather high altitudes. Here we focus on altitudes <2 km, for which MAX-DOAS observations are most sensitive. At these altitudes, the horizontal sensitivity ranges are <83 km (1° elevation angle), <52 km (2° elevation angle), and <36 km (3° elevation angle). Thus we limit this exercise to horizontal sensitivity ranges <80 km. Note that horizontal sensitivity ranges >40 km only occur for very low aerosol optical depths (<0.005). For such distances, also the effect of the earth's curvature is small (<130m).

In the following we consider elevation angles of 1°, 2°, and 3°, for which the horizontal sensitivity ranges for atmospheric layers below 2 km is largest.

In Figure 13 relationships between the retrieved O_4 DSCDs and the horizontal sensitivity ranges derived from radiative transfer simulations are shown. The results are obtained for a fixed SZA of 60°, relative azimuth angles of 0°, 90°, and 180°, and for different aerosol layer heights. Results for elevation angles of 1° and 3° and wavelengths of 360 nm and 630 nm are shown. The blue lines indicate polynomial fits (degree 2) to the results for an aerosol profile extending from 0-2000m, which can be used as upper limit for the horizontal sensitivity range. Polynomial coefficients for these results and also for additional wavelengths and elevation angles are presented in the table below. Although the radiative transfer simulations were performed for a fixed SZA of 60°, they are roughly representative for SZA < 70°.

Finally it should be noted that there is a clear geometric relationship between the height and horizontal distance of the air mass, for which MAX-DOAS observations are sensitive. These relationships depend on elevation angle (see Figure 14 below).

360 nm, 1°

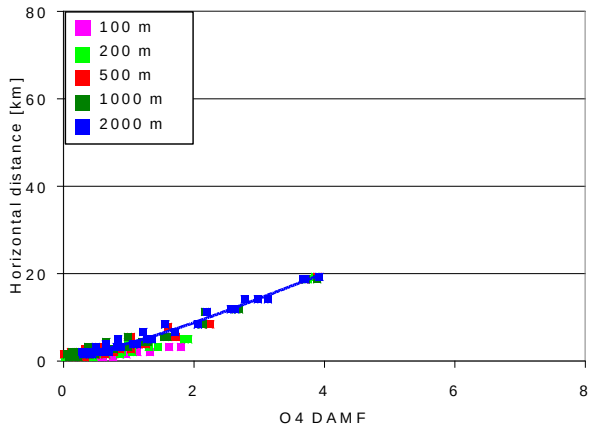

360 nm, 3°

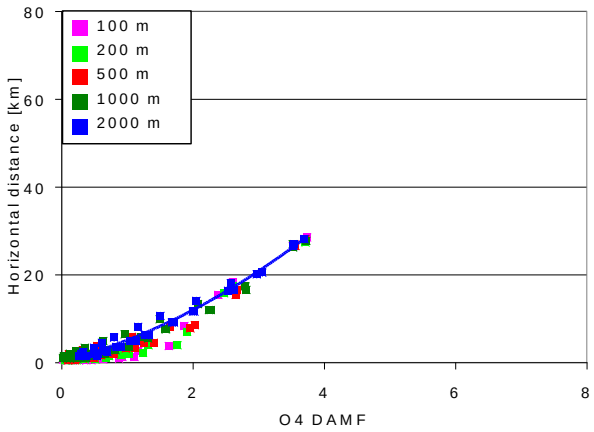

630 nm, 1°

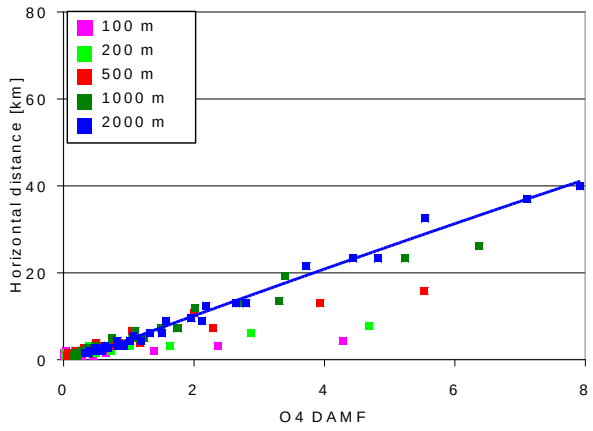

630 nm, 3°

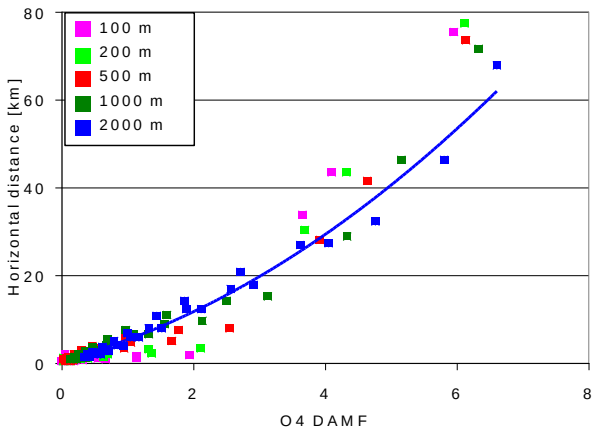

Figure 13. Relationships between the retrieved O4 DSCD and the horizontal sensitivity range for selected elevation angles and wavelengths (SZA: 60°: relative azimuth angles: 0°, 90°, 180°). The different colours represent results for different aerosol extinction (box) profiles.

Polynomial coefficients ($y = ax^2 + bx + c$) for different wavelengths and elevation angles derived from the fit to the radiative transfer results for an aerosols layer 0 - 2000m. (SZA: 60°: relative azimuth angles: 0°, 90°, 180°)

wave-length	pol. coefficients a	b	c	pol. coefficients a	b	c	pol. coefficients a	b	c
360 nm	0.409	3.339	0.380	0.607	3.780	0.107	1.009	3.822	0.255
477 nm	0.101	4.676	0.301	0.211	5.304	0.606	1.076	2.916	1.214
577 nm	0.008	5.257	0.782	0.133	5.792	0.977	0.922	3.502	0.874
630 nm	-0.036	5.588	1.000	0.106	5.988	1.092	0.807	3.960	0.588

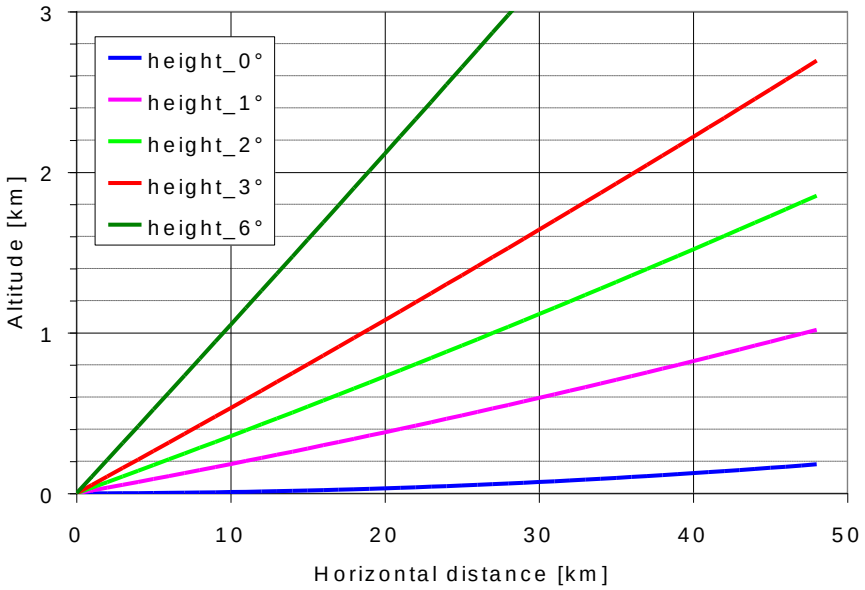

Figure 14. Relationships between altitude and horizontal distance of an air mass observed by MAX-DOAS observations for different elevation angles. The effect of the earth's curvature is taken into account.

F. References

Clémer, K., Van Roozendael, M., Fayt, C., Hendrick, F., Hermans, C., Pinardi, G., Spurr, R., Wang, P., and De Mazière, M.: Multiple wavelength retrieval of tropospheric aerosol optical properties from MAXDOAS measurements in Beijing, Atmos. Meas. Tech., 3, 863-878, 2010.

Connor, B. J., Siskind, D. E., Tsou, J. J., Parrish, A., and Remsberg, E. E.: Ground-based microwave observations of ozone in the upper stratosphere and mesosphere, J. Geophys. Res., 99 (D8), 16,757-16,770, 1994.

Eskes, H. J., and Boersma, K. F.: Averaging kernels for DOAS total-column satellite retrievals, Atmos. Chem. Phys., 3, 1285–1291, 2003.

Frieß U., Monks, P.S., Remedios, J.J., Rozanov, A., Sinreich, R., Wagner, T. and Platt, U.: MAX-DOAS O_4 measurements: A new technique to derive information on atmospheric aerosols: 2. Modeling studies, J. Geophys. Res. 111, D14203, doi:10.1029/2005JD006618, 2006.

Rodgers, C. D.: Inverse Methods for Atmospheric Sounding, Theory and Practice. World Scientific Publishing, Singapore-NewJersey-London-Hong Kong, 2000.

III. Ozone Microwave Radiometry

A. Intro (general)

A.1 Instrument fiche

Table 5. Ozone Microwave Radiometry, instrument fiche

Platform	ground-based
Measuring technique	passive, pressure broadened emission line
Observation geometry	uplooking, typically 20-40◦ elevation
Units	Volume mixing ratio (vmr)
Vertical resolution	10-20 km, increasing with altitude
Horizontal resolution	Field of view typically 6 degree
Temporal resolution	30 min - 60 min (integration of 20-sec line spectra)
Vertical range	20-70 km
Horizontal range	about 5x5km at 50 km
Stability/ drift	avoided by calibration with a cold and hot load
Precision	5% @40 km, 10% @60 km (based on satellite validation)
Systematic uncertainty	5-10%
Daytime/ nighttime	independent of day- or nighttime
Weather conditions	not critical, unless severe humidity or precipitation
Interferences/ contamination (payload, spectral)	electromagnetic interference from communication signals
Bottlenecks, limitations	high tropospheric humidity
Absolute or calibration needed?	Calibration with liquid nitrogen needed in regular intervals
Corrections needed?	no
Auxiliary data	Temperature profiles from radiosondes and/or Re- analysis
Averaging kernels	Important component of the produced data: give information about measurement and a priori content
A priori information	a priori info for ozone needed e.g. from climatology
Spectroscopic parameters	from spectroscopic databases (JPL and HITRAN)
Transportability/ Suitability for campaign	Compact systems exist soon for campaigns
System availability	n/a
Data processing time	n/a
Additional products	opacity at the used microwave frequency
Future potential	traveling standard (compact instrument for validation campaigns), cheaper technology allowing to build more instruments
Caveats	Averaging kernels required for proper interpretation

* Table is similar to Fact sheets in Kämpfer (2013)

A.2 Measurement technique

Ozone microwave radiometers are operated indoors. The microwave radiation of the atmosphere passes through the blue styrofoam window.

Figure 15. A typical ozone microwave radiometer (GROMOS at Bern)

Figure 15 shows a typical ozone microwave radiometer (GROMOS at Bern). The brightness temperature of the atmosphere is calibrated by means of a cold load. A vessel with liquid nitrogen provides a black body brightness temperature of 80 K. A FFT spectrometer records the pressure-broadened ozone line spectra at 142 GHz with a bandwidth of 1 GHz.

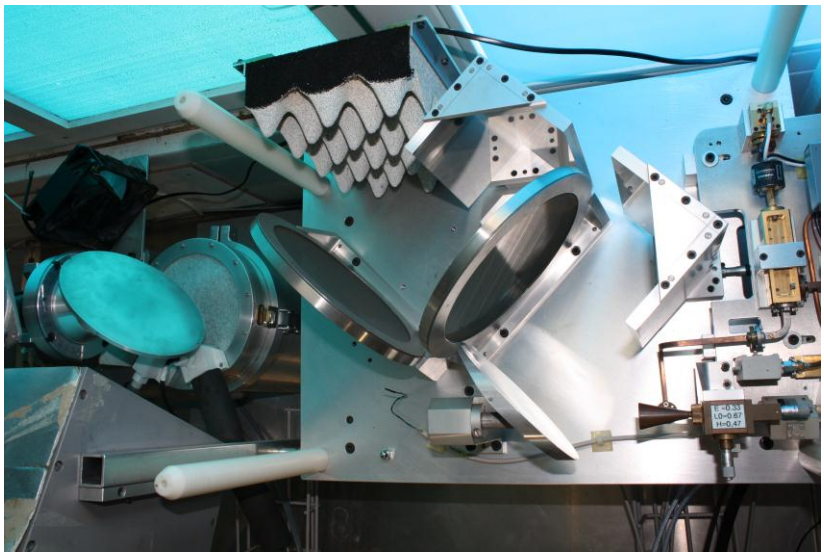

Figure 16. Frontend with quasi optics of the microwave radiometer.

Figure 16 shows a frontend with quasi optics of the microwave radiometer. Rotating aluminum plate mirror (left-hand-side), Martin-Puplett Interferometer with wire grids and corner mirrors (middle), a copper horn antenna, wave guides, and mixers (right-hand-side).

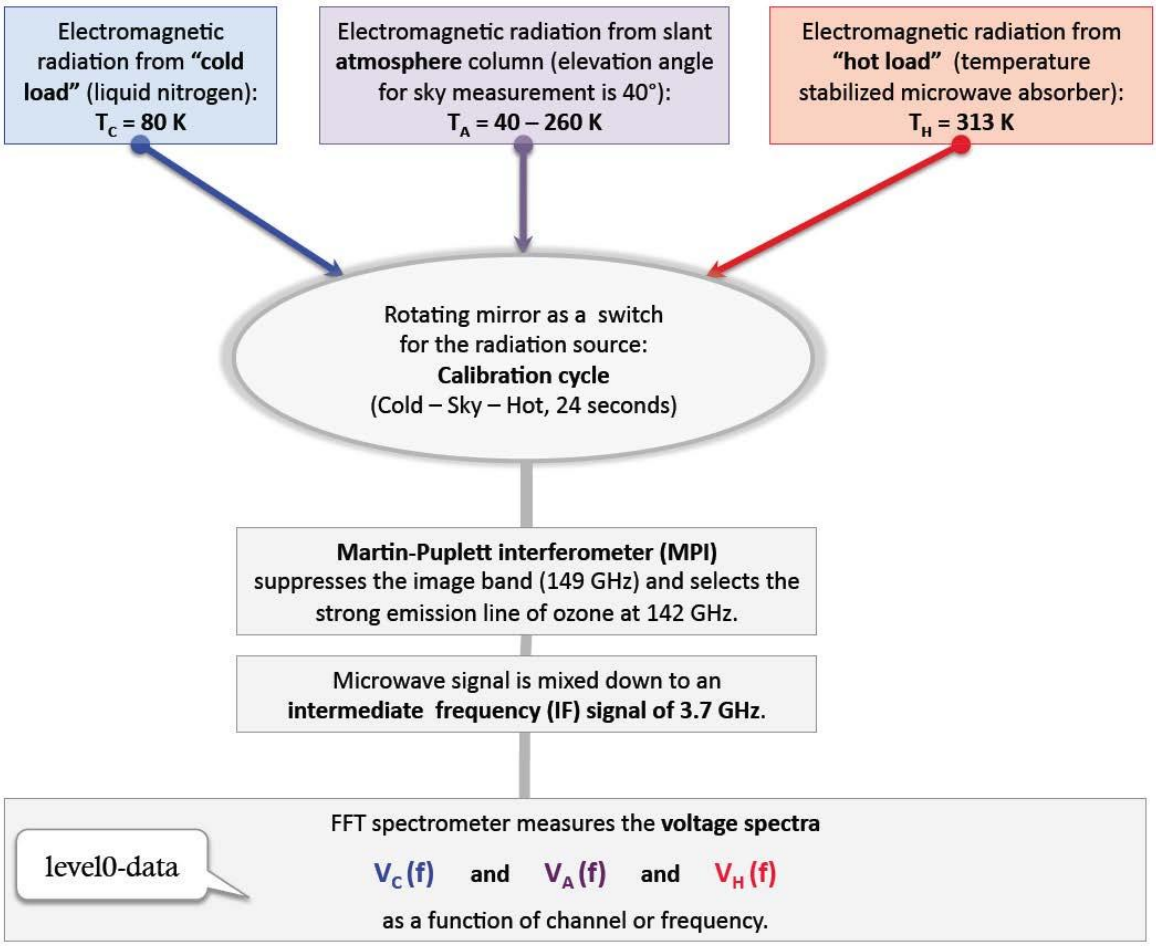

Figure 17. Flow chart of the measurement process

The ozone microwave radiometer provides three voltage spectra: cold load, hot load, and the atmosphere with a strong ozone emission line. These data are the level0 data.

A.3 Data analysis

From voltage spectra (level-0) to vertical ozone profiles (level-2)

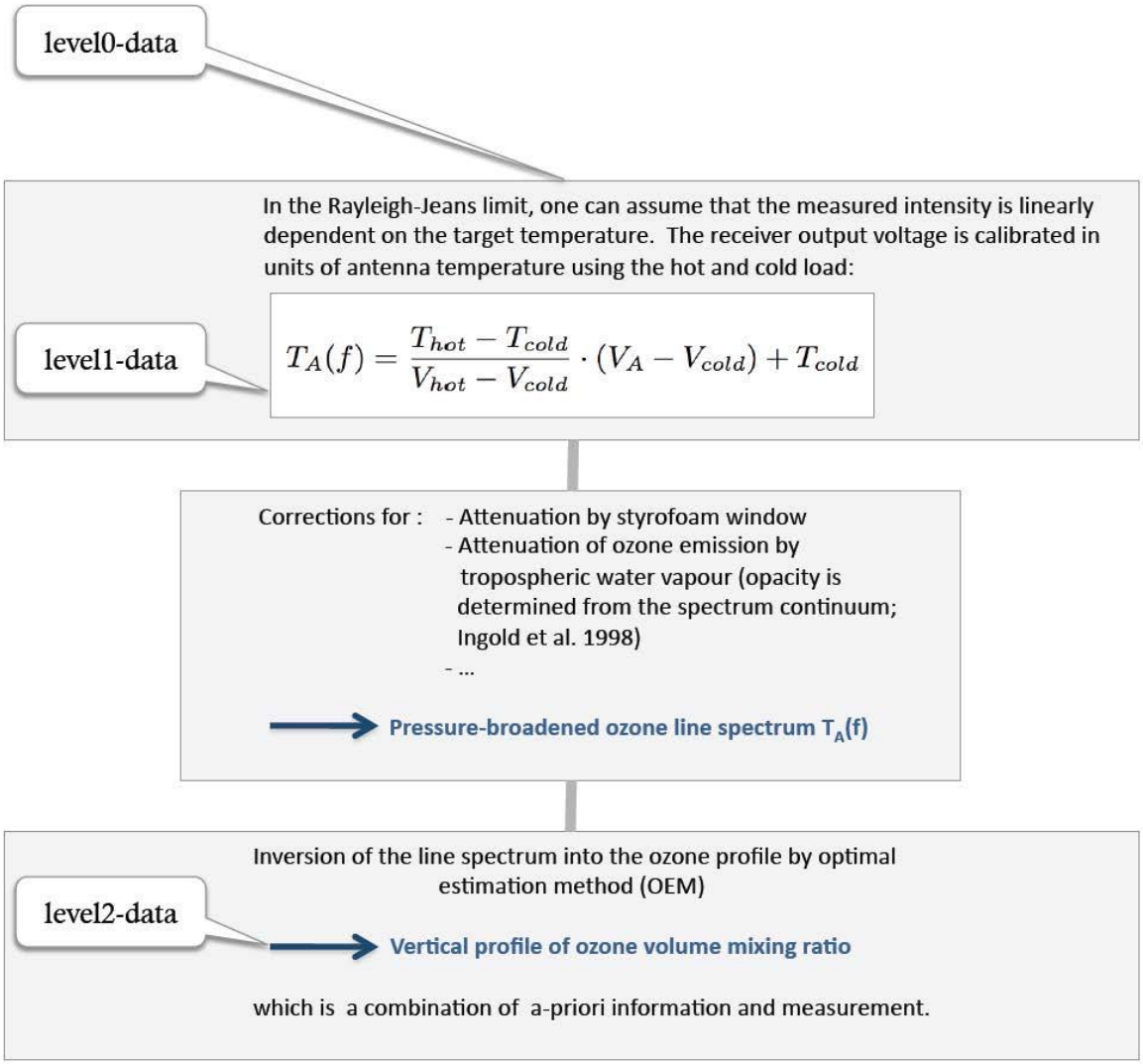

Figure 18. Flow chart of the data retrieval.

Figure 18 shows a flow chart of the data retrieval. The retrieval chain can slightly change from institute to institute, e. g., in case of OZORAM the water vapour continuum is simulated by means of radiative transfer and an apriori profile.

B. Ozone microwave radiometers of NORS: GROMOS and OZORAM

B.1 GROMOS (Ground-based Millimeter-wave Ozone Spectrometer)

B.1.a. Instrument fiche

Table 6. GROMOS, instrument fiche

Location	Bern, Switzerland
Latitude, Longitude, Altitude	46.95°N, 7.44°E, 577m
Direction of view	North-East
Elevation of antenna	40°
Mode of Operation	Total power
Temperature of Mixer	~ 294 K (uncooled, room temperature)
System noise temperature	~ 2520 K
Frequency of ozone line	142.17504 GHz
Target species	O_3
aux. Quantities	Opacity
Altitude Range of target species	25 - 70 km
Time resolution	30 min (FFTS), 60 min (filter bench)
Spectrometer	48-channel filter bench (1994-2011), 32768-channel FFT spectrometer (since 2009)

B.1.b. Operation mode

GROMOS measures automatically. The operator can remotely check the instrumental performance (LabView). The dewar with liquid nitrogen has to be refilled 2-3 times per week by the operator.

GROMOS operates in Total Power mode. Calibration is performed by switching between a hot load at 312 K, a cold load at 80 K (liquid nitrogen), and the atmospheric target. The cycle is repeated every 24 seconds as shown in Figure 17. A 48-channel filter bench was used from 1994 to 2011. The overall bandwidth was 1.2 GHz with a resolution of about 200 kHz in the line center. Since September 2009, a 32768-channel FFT spectrometer yields the ozone spectra with a high resolution (30 kHz) over the whole bandwidth. Both spectrometers were operated parallel between 2009 and 2011 in order to have an overlap.

The raw data, called L0-data, are stored as binary files on a dedicated data RAID, which also serves as a backup. Additionally to the binary-files, auxiliary information such as temperatures measured by sensors in the GROMOS room, various voltages of the instrument (giving for example the exact mirror position) are stored in text files.

B.1.c. L1 data

The L1 data are the frequency and power calibrated spectra. The calibration is performed offline as well as the retrieval. The L1 data are calculated using the total power formula and the measured temperatures of the hot and cold black body. The L1 data are calibrated and temporally integrated: For the standard retrieval, one spectrum is available per 30 minutes. The calibrated spectra are further binned (averaged in the frequency range), resulting in a frequency resolution of 30 kHz around the line center and a frequency resolution of approximately 80 MHz at the wings.

B.1.d. L1 -> L2 data

The L1 spectra of brightness temperature are inverted into vertical profiles of ozone volume mixing ratio. These so-called L2-data, profiles together with necessary retrieval data, are transferred to a MySQL database at the University of Bern.

The retrieval uses the ARTS/QPACK (version 2.0) software package, which is dedicated to measurements in the millimeter-wave region (Eriksson et al., 2011). QPACK is an implementation of the optimal estimation method to invert ill-posed functions (Eriksson et al., 2005).

There is a "tropospheric correction" which takes the absorption of the stratospheric ozone emission by tropospheric water vapour into account. The tropospheric correction is described by Peter (1997) and Ingold et al. (1998). Tropospheric opacity at 142 GHz is a spin-off of the tropospheric correction. ECMWF reanalysis and meteorological station data are used as auxiliary data. The ozone apriori climatology is a mixture of an ozone climatology of Aura//MLS, ECMWF reanalysis, and previous GROMOS ozone profiles.

B.1.e. L2 data use and caveats

The retrieved data are marked valid using the following conditions:

1. retrieval has converged
2. tropospheric attenuation is less than 0.7
3. check of the ozone profiles by a scientist (filter bench produced more runaway ozone profiles than the FFTS)

The averaging kernel matrix and the a priori profile are saved with the retrieved profile. The averaging kernel matrix describes the vertical averaging that should be used if the GROMOS measurements are compared to independent measurements or model data. The horizontal averaging over the field of view is considered negligible and not taken into account.

B.1.f. References

IAP-Bern reports can be downloaded at http://www.iap.unibe.ch/publications.

P. Eriksson, Buehler, S., Davis, C., Emde, C., and Lemke, O., 2011, ARTS, the atmospheric radiative transfer simulator, version 2, Journal of Quantitative Spectroscopy and Radiative Transfer, 112, 1551□1558, ISSN 00224073, doi:10.1016/j.jqsrt.2011.03.001.

P. Eriksson, Jiménez, C., and Buehler, S. A., 2005, Qpack, a general tool for instrument simulation

and retrieval work, J. Quant. Spectrosc. and Radiat. Transfer, 91, 47□64, doi:10.1016/j.jqsrt.2004.05.050.

C. Dumitru, K. Hocke, N. Kämpfer, Y. Calisesi: Comparison and validation studies related to ground-based microwave observations of ozone in the stratosphere and mesosphere, *Journal of Atmospheric and Solar-Terrestrial Physics*, ed.: Elsevier, vol.: 68, no.: 7, pp.: 745-756, 2006

K. Hocke: Homogenisation of the ozone series of the microwave radiometers SOMORA and GROMOS, IAP Research Report, No. 2007-04-MW, Institut für angewandte Physik, Universität Bern, 2007

K. Hocke: Comparison of Ozone Measurements by GROMOS, SOMORA, Aura-MLS, and Ozonesonde, IAP Research Report, No. 2005-04-MW, Institut für angewandte Physik, Universität Bern, 2005

T. Ingold, Peter R., Kämpfer N.: Weighted mean tropospheric temperature and transmittance determination at millimeter-wave frequencies for ground-based applications, Radio Science, vol.: 33, no.: 4, pp.: 905-918, 1998

N. Kämpfer: Monitoring Atmospheric Water Vapour: Ground-Based Remote Sensing and In-situ Methods, ed.: Niklaus Kämpfer, vol.: 10, series: ISSI Scientific Report Series, Springer New York, http://dx.doi.org/10.1007/978-1-4614-3909-7, 2012, ISBN 978-1-4614-3908-0, 2013

R. Peter: The Ground-based Millimeter-wave Ozone Spectrometer - GROMOS, IAP Research Report, No. 1997-13, Institut für angewandte Physik, Universität Bern, 1997

B.2. OZORAM

B.2.a. Instrument fiche

Table 7. OZORAM, instrument fiche

Location	Ny Ålesund, Spitsbergen, Norway
Latitude, Longitude, Altitude	78.9,11.9,15m
Direction of view (AZIMUTH, Elevation)	113°, 20°
Mode of Operation	Total power
Temperature of Mixer	60K
System noise temperature	1200 K
Frequency	142.175 GHz
Target species	O3
aux. Quantities	Water vapour column
Altitude Range of target species	30 - 75 km
Time resolution	60 min

B.2.b. Operation mode

OZORAM measures semi-automatically. The operator checks the instrumental features and fills in a protocol every day.

The OZORAM operates in Total Power mode, i.e. a hot, H, (ambient temperature) and a cold load, C, (60 K, cryogenically cooled along with the mixer) measured alternatively with the sky, A, in a ratio (H:A:C = 50:44:6) in order to produce the highest signal to noise ratio at a sky temperature of about 80K. The cold load is a cryogenically cooled black-body which is calibrated/checked once a week using a black body cooled with liquid nitrogen.

The raw data, called L0, are transferred to the University of Bremen, where they are stored along with all data necessary to calibrate the spectra and secured on a dedicated computer system. The granularity of the raw data is about 10 min, which is also the highest time resolution the OZORAM measurements could have in the current setup.

B.2.c. L1 data

The L1 data are the frequency and power calibrated spectra. The calibration is performed offline as well as the retrieval. The L1 data is calculated using the total power formula and the measured temperatures of the hot and cold black body.

B.2.d. L1 -> L2 data

The calibrated L1 spectra are integrated further to reach a time resolution of 60 minutes. This time resolution is a compromise between a high time resolution and a signal to noise ratio sufficient to retrieve a profile up to the physical limit at about 75 km altitude. The physical limit is defined by the properties of the radiation at this frequency in this viewing geometry and cannot be raised.

The retrieval uses the ARTS/QPACK software package, which is dedicated to measurements in the millimeter-wave region. QPACK is an implementation of the optimal estimation method to invert ill-posed functions.

There is no "tropospheric correction", i.e. contrary to most instruments the tropospheric contribution is not estimated and removed from the measured spectrum. The tropospheric absorption is fitted along with the O_3 profile.

Because the OZORAM is affected by wavelike structures on the spectrum, the retrieval also fits a number of standing waves along with the profile. This is the reason while the lower boundary of the altitude range is 30 km, not below 20 km as theory would predict.

The noise on the spectrum is calculated using the system noise temperature and used as a fit parameter. The a priori profile and the auto-covariance matrix are fixed.

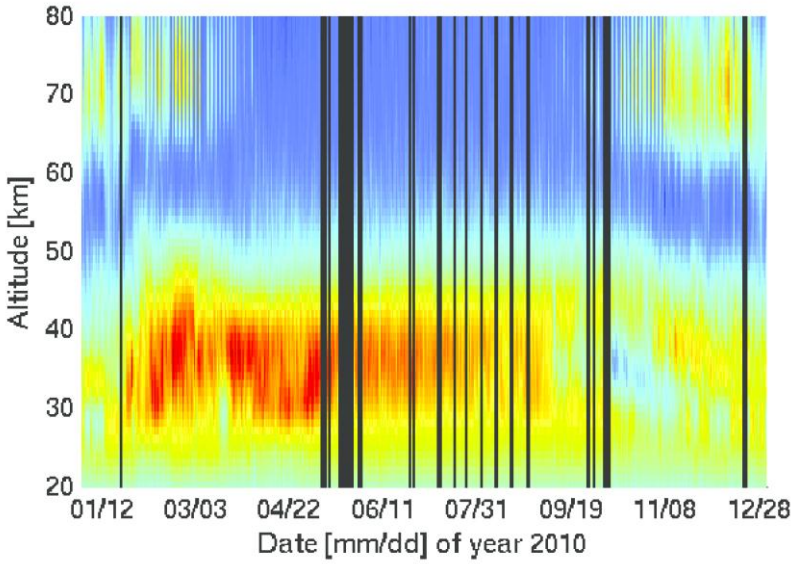

Figure 19. Time series of strato-mesospheric Ozone measured using the OZORAM

B.2.e. L2 data use and caveats

The retrieved data are marked valid using the following conditions:

1. retrieval has converged
2. line center of the O_3 emission is properly fitted, failure to do so points to an instability in the system
3. the atmospheric background is below 200 K
4. the standing waves are below 10 times of the noise level
5. the retrieved water vapour column is positive
6. there are no strong negative overshoots in the retrieved profile

The averaging kernel matrix and the a priori profile are saved with the retrieved profile. The averaging kernel matrix describes the vertical averaging that should be used if the OZORAM measurements are compared to independent measurements or model data. The horizontal averaging over the field of view is considered negligible and not taken into account.

B.2.f. References

For more information and examples compare

Palm, M.; Hoffmann, C. G.; Golchert, S. H. W. & Notholt, J. The ground-based MW radiometer OZORAM on Spitsbergen -- description and status of stratospheric and mesospheric O_3-measurements, Atmos. Meas. Tech., 2010, 3, 1533 – 1545.

Palm, M.; Melsheimer, C.; Noël, S.; Heise, S.; Notholt, J.; Burrows, J. & Schrems, O. Integrated water vapor above Ny Ålesund, Spitsbergen: a multi-sensor intercomparison, Atmos. Chem. Phys, 2010, 10, 1-12.

IV. Ozone DIAL

A. Instrument fiche

Table 8. Ozone DIAL, instrument fiche

Instrument	The O_3 lidar (Light Detection and Ranging) is an active remote sensing instrument
Platform	Ground-based
Measuring technique	Differential Absorption Laser technique (DIAL) which requires the simultaneous emission of two laser beams
Observation geometry	zenith
Units	O_3 number density profiles (mol/cm^3), volume mixing ratio profiles(vmr), partial column (mol/cm^2)
Vertical resolution	Increasing from ~0.5 km at 20 km to ~6 km at 50 km
Horizontal resolution	Depending on the power and the repetition rate of the laser, an ozone measurement lasts typically four hours, leading to a spatial resolution of the order of 200 km, depending on the atmospheric wind conditions
Temporal resolution	~4 hours of measurements
Vertical range	10 -50 km
Horizontal range	none
Stability/drift	Lidar ozone measurements are self-calibrated. Long-term drift with respect to other measurement time series show values close to zero at most altitudes (Nair et al ., 2012)
Precision	from ~1% at 20 km to 10%-50% at 50 km depending on the systems and the weather conditions
Systematic uncertainty	~0.5% at 10 km to about 4% at 30 km and ~ 5 % in the upper stratosphere
Daytime/ nighttime	Nighttime
Weather conditions	lidar measurements require clear sky conditions since laser radiation is rapidly absorbed by clouds. Only cirrus can be tolerated for accurate stratospheric ozone measurements.
Interferences/ contamination (payload,	None

spectral)	
Bottlenecks, limitations	Large, heavy and expensive instrument; When placed in a container, lidars can be transported.
Absolute or calibration needed?	Self-calibrating technique: no need of instrumental constants.
Corrections needed?	No
Auxiliary data	Pressure / Temperature profiles from local observations or model
Averaging kernels	None
A priori information	None
Spectroscopic parameters	O_3 cross section from Bass and Paur (1985) is presently used. Future change of ozone cross section is considered depending on IGACO – O3 recommendation
Transportability/ Suitability for campaign	Transportable if placed in a large container
System availability	Commercial laser and data acquisition system, lab made optical receiving system (telescope and spectrometer), lab made
Data processing time	L2 data are produced the day following the measurement.
Additional products	Temperature profile retrieved from the off-wavelength signal
Future potential	Aerosol backscatter profile
Caveats	The lower limit and upper limit of the ozone profile depend on the laser power and the meteorological conditions.

B. Operation mode

The lidar is a remote sensing instrument. Depending on the desired measurement, lidar systems use various light-matter interactions such as Rayleigh, Mie and Raman scattering or fluorescence. Measurements of atmospheric ozone, temperature or aerosol are based on the first 3 processes. Generally, a lidar measurement consists in sending into the atmosphere a laser beam; a small part of this laser radiation is scattered back to the ground, where it is collected by a telescope, detected by a photomultiplier tube and analysed by an electronic acquisition system. Range resolved measurements can be obtained using pulsed lasers. In order to measure the ozone vertical distribution, the DIfferential Absorption Laser technique (DIAL) is used. This technique requires the simultaneous emission of two laser beams characterised by a different ozone absorption cross-section.

A lidar system includes basically one or several laser sources with optical devices to reduce the divergence of the beam, a telescope which collects the light scattered back by the atmosphere, an optical analysing system with detectors such as photomultipliers to detect the optical signal, and an electronic acquisition system. The analysing systems used to digitize the electronic signal provided by the photomultipliers include photon counting and/or transient analysers (cf figure 20).

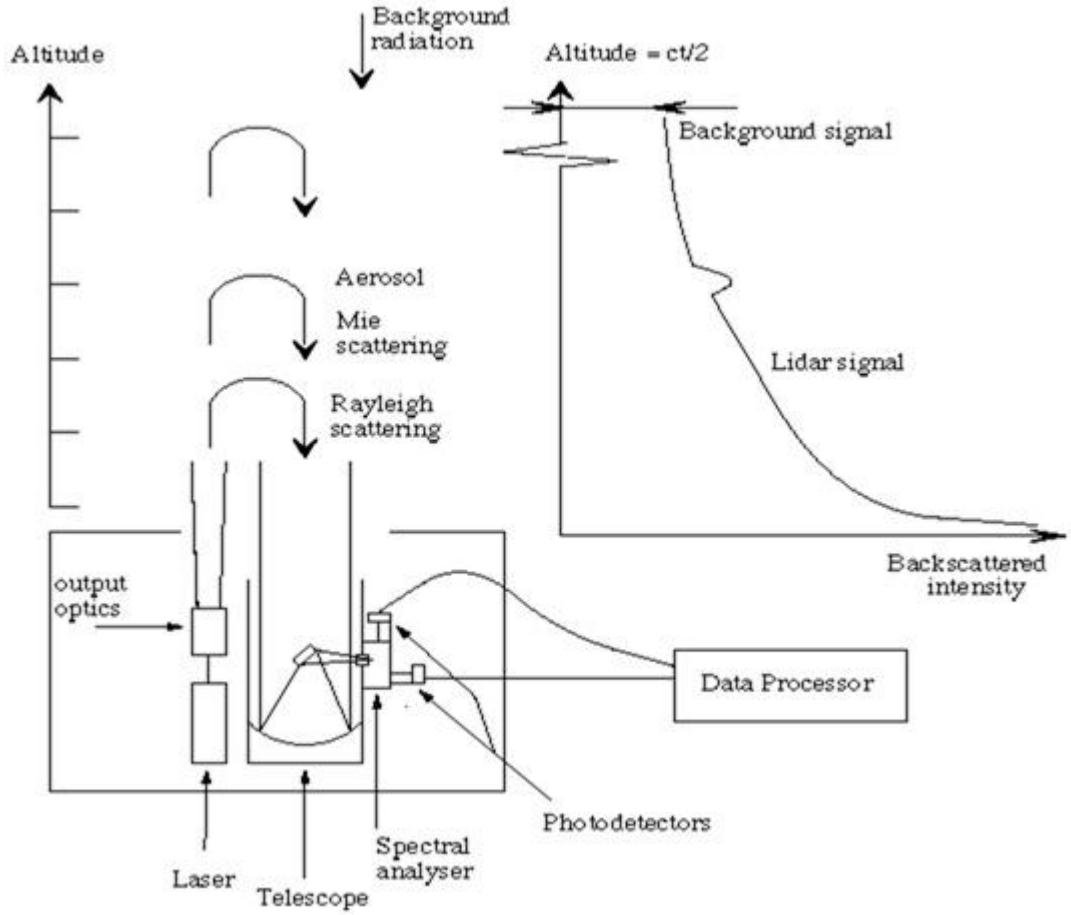

Figure 20. Schematic view of the principle of a lidar system.

In the case of DIAL systems using the emission of two laser wavelengths, the optical receiving system comprises spectral analyzing optics, such as interference filters or spectrometers.

The DIfferential Absorption Lidar (DIAL) technique uses the absorption properties of a given atmospheric constituent to deduce its atmospheric concentration. Laser beams at two different wavelengths are sent into the atmosphere. The wavelengths are chosen so that one of them is significantly more absorbed (wavelength "ON") than the other (wavelength "OFF"). The difference in the absorption along the beam path causes the returned lidar signals to yield a different altitude dependence. Knowing from laboratory work the absorption cross-sections of the constituent at both wavelengths, the atmospheric number density of this constituent can be deduced from the slope of the logarithm of the ratio of the signals at the two wavelengths. This technique does not require any calibration.

To monitor atmospheric ozone with the DIAL technique, the choice of the laser wavelengths depends on the altitude range of the measurement. The spectral range is chosen first in the ultraviolet where the ozone absorption is more efficient, but the selected wavelengths differ according to whether the measurement is made in the troposphere or in the stratosphere - for stratospheric measurements, the objective is to reach the stratosphere and to detect the high ozone concentrations there (Browell, 1989, Papayannis *et al.*, 1990). Furthermore, in the higher stratosphere, one has to consider the simultaneous decrease of the ozone number density and the atmospheric number density which provides the

backscatter radiation. This leads to the need for powerful laser sources in order to reach the high altitude ranges. The absorbed wavelength should not be strongly absorbed in order to reach the stratosphere. Most teams working on this subject use XeCl eximer laser sources, which emit directly in the UV at 308 nm (Uchino *et al.*, 1978) and are very powerful (100 W are commonly reached with the present systems). For the non-absorbed wavelength, different techniques are used, mainly the generation of a wavelength at 353 nm corresponding to the first Stokes radiation by stimulated Raman effect in a cell filled with hydrogen (Werner *et al.*, 1983), the use of the third harmonic of a Nd:Yag laser (355 nm) (Godin *et al.*, 1989), or the use of a XeF laser which provides a wavelength at 351 nm (Nakane *et al.*, 1994).

Lidar measurements are performed during nighttime and require clear sky meteorological conditions - laser radiation is rapidly absorbed by clouds and only cirrus can be tolerated for accurate stratospheric measurements.

The DIAL algorithm follows basically the theoretical derivation of the ozone number density from the lidar signals. The main steps are the following:

- Temporal signal averaging
- Correction from:
  - ✓ background light
  - ✓ dead time correction in the case of photon counting acquisition, due to the saturation of the photon counting systems with high intensities.
- Derivation of the ozone number density from the corrected lidar signals

C. L1 data

In the routine mode, the lidar signals are time-averaged over the whole measurement period (3–4 h in general) in order to increase the signal-to-noise ratio (cf figure 21).

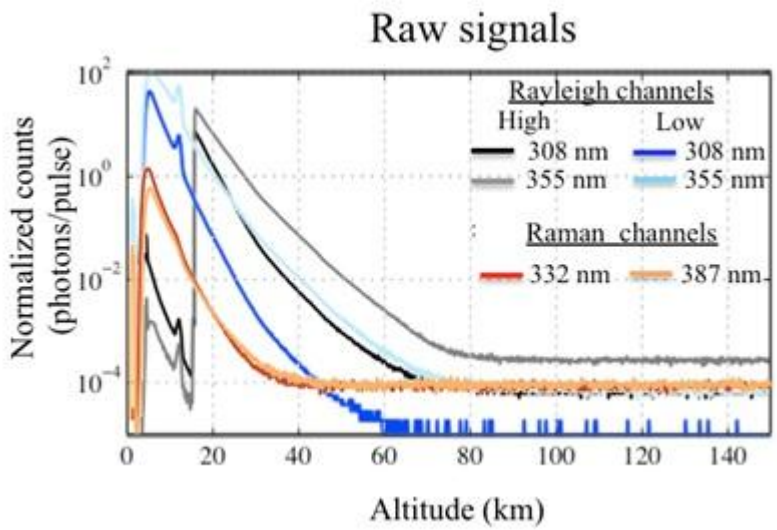

Figure 21. Temporal signal averaging in order to increase the signal-to-noise ratio.

D. L1 ->L2 data processing principles

Several corrections are applied to the averaged signal, such as the background correction in which the background light is estimated using a linear regression in the altitude range where the lidar signal is negligible (80–150 km), and the dead-time correction effect in order to account for the saturation of the photon counting signals in the lower ranges.

The ozone number density is retrieved from the derivation of the logarithm of the corrected lidar signals according to the following equation:

$$n_{o3} = \frac{-1}{2\,\Delta\sigma_{o3}(z)}\frac{d}{dz}\ln\left(\frac{P(\lambda_1,z)-P_{b1}}{P(\lambda_2,z)-P_{b2}}\right)+\delta n_{o3}(z)$$

where nO3(z) is the ozone number density at altitude z, $P(\lambda_i,z)$ is the number of detected photons at wavelength λ_i backscattered from altitude z, P_{bi} is the background radiation at wavelength λ_i, and $\Delta\sigma_{O3}(z)$ corresponds to the differential ozone absorption cross-section $\sigma_{O3}(\lambda_1,z)$- $\sigma_{O3}(\lambda_2,z)$. Ozone absorption cross-sections depend on atmospheric temperature and thus on altitude. $\delta n_{O3}(z)$ is a correction term depending on absorption by other constituents and Rayleigh and Mie differential extinction and scattering. $\delta n_{O3}(z)$ is expressed as follows

$$\delta n_{o3}(z) = \frac{1}{\Delta\sigma_{o3}(z)}\left[\frac{1}{2}\frac{d}{dz}\ln\left(\frac{\beta(\lambda_1,z)}{\beta(\lambda_2,z)}\right)-\Delta\alpha(z)-\sum_e \Delta\sigma_e n_e(z)\right]$$

where $\beta(\lambda_i,z)$ is the total atmospheric backscatter coefficient at wavelength λ_i and altitude z, $\Delta\alpha(z)$ is the differential atmospheric extinction $\alpha(\lambda_1,z) - \alpha(\lambda_2,z)$ linked to Rayleigh and Mie scattering and $\sum_e \Delta\sigma_e n_e(z)$ the differential extinction by other atmospheric compounds. In the DIAL technique, the laser wavelengths are chosen so that the term $\delta n_{o3}(z)$ represents less than 10% of the term derived from the slope of the lidar signals in the altitude range of interest. The derivation of the ozone number density from the laser signals shows thus that the DIAL technique is a self-calibrated technique which does not need the evaluation of instrumental constants.

The ozone number density is derived from the three lidar signal pairs detected by the experimental system: Rayleigh high-energy, Rayleigh low-energy and Raman, which optimizes the accuracy of the retrieved ozone profile in the high stratosphere, the middle-low stratosphere and the lower stratosphere respectively. In condition of background stratospheric aerosol, it is preferable to use the low-energy Rayleigh signals in the lower stratosphere, since they provide a better vertically resolved ozone profile than the Raman signals. The use of these signals in the lowermost stratosphere is prevented by the saturation of the photon counters, as is the use of the high-energy Rayleigh signals higher up. A method based on the adjustment of the parameter used for the pulse pile-up correction was then designed, in order to optimize the range where the most energetic lidar signal pair can be used, improving thus the precision of the final ozone profile. The equation used to compute the true photon count rate from the observed count rate is the following, derived from the Poisson statistics:

$$P_c = 1 + \big((1-x)P_r - 1\big)\exp(-xP_r)$$

where P_c is the observed photon count rate, P_r is the true count rate and $x \sim 1/P_{max}$ with P_{max} being the maximum observed count rate. In the case of the high-energy Rayleigh signals, the parameter x used for the pulse pile-up correction is adjusted for each wavelength in order to obtain the best agreement

between the slopes of both low-energy and high-energy Rayleigh signals. For the low-energy Rayleigh signals, we use the Raman signals by computing 'reference Rayleigh' slopes from the Raman signal slopes, the derived Raman ozone profile and the Rayleigh extinction correction. With this technique, the best agreement between the ozone profiles derived from the various wavelength pairs is obtained. The final ozone profile is retrieved, first, by combining for each wavelength the slopes of the low-energy and high-energy Rayleigh signals, and then, by combining the Raman and the composite Rayleigh ozone profiles. The altitude range where both profiles are combined depends on the stratospheric aerosol content. The monitoring of the aerosol content in the stratosphere is made by computing the backscatter ratio (defined as the ratio of the total backscatter coefficient to the Rayleigh backscatter coefficient) at 355 nm, using the Klett method. This allows us to check the presence of aerosol layers due to small volcanic eruptions reaching the lower stratosphere or the presence of subvisible cirrus. In background aerosol conditions, the combination of the Rayleigh and Raman ozone profile is made around 14– 15 km. Finally, both the Raman and composite Rayleigh profiles are corrected from the Rayleigh extinction using composite pressure–temperature profiles.

E. L2 data and use caveats (hdf)

In addition to the number density profiles, the data files also provide the volume mixing ratio profiles, the integrated profiles or total columns in the valid domain. With each variable, the associated random, systematic and total uncertainty is provided – see Guide to Data Uncertainties.

At OHP station:

- ✓ For each ozone profiles, the user must take the data in the valid domain defined in the metadata and "variable note" in the HDF files.
- ✓ Pressure and Temperature profiles used for the ozone retrieval are a composite of various models.
  For NRT data: Daily P and T from Arletty model
  For consolidated data: Daily P and T from local sounding + NCEP + MAP85

At Reunion station:

- ✓ For each ozone profiles, the user must take the data in the valid domain defined in the metadata and "variable note" in the HDF files.
- ✓ Pressure and Temperature profiles used for the ozone retrieval are a composite of various models.
  For NRT data: Daily P and T from Arletty model
  For consolidated data: Daily P and T from local sounding + ECMWF + MAP85

F. Including concept/examples of horizontal/vertical averaging

Depending on the power and the repetition rate of the laser, an ozone measurement lasts typically several hours, leading to a spatial resolution of the order of 100 km, depending on the atmospheric conditions. Due to the rapid decrease of the signal to noise ratio in the high stratosphere, it is necessary to degrade the vertical resolution of the measurement in order to limit the statistical error at this altitude range, to reasonable values. In the DIAL technique, it is necessary to use a low-pass filter in order to account for the rapid decrease of the signal-to-noise ratio in the high altitude range. In our case, the logarithm of each signal is fitted to a 2^{nd} order polynomial and the ozone number density is computed from the difference of the derivative of the fitted polynomials. The smoothing is achieved by varying the number of points over which the signals are fitted. The resolution is calculated from the

cut-off frequency of the low-pass filter defined at 23 dB. The relation between the filter cut-off frequency and the number of points used was obtained empirically by calculating the filter transfer function for various filter orders. The DIAL stratospheric ozone lidar profiles are thus generally characterized by a vertical resolution varying from several hundred meters in the lower stratosphere, to several kilometers around 50 km (cf. Figure 22, (Godin et al., 1999)). The information about the vertical resolution is provided in the HDF files in the variable O3.NUMBER.DENSITY_ABSORPTION.DIFFERENTIAL_RESOLUTION.ALTITUDE.ORIGINATOR.

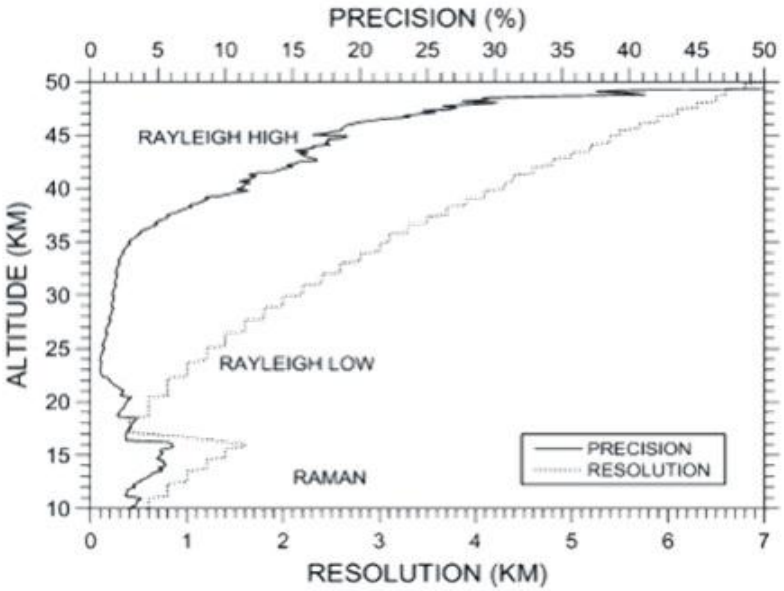

Figure 22. Precision and vertical resolution profile of an ozone measurement in the case of the OHP (Observatoire de Haute Provence –in France) lidar instrument. Both the precision and the vertical resolution profile depend on the experimental configuration. The precision can vary from one measurement to the other.

G. References

E. V. Browell, Proc. IEEE, 1989, 77, 419–432.

A. Papayannis, G. Ancellet, J. Pelon and G. Mégie, Appl. Opt., 1990, 29, 467–476.

O. Uchino and I. Tabata, Appl. Opt., 1991, 30(15), 2005.

J. Werner, K. W. Rothe and H. Walther, Appl. Phys. B., 1983, 32, 113–118.

Bass AM, Paur RJ. The ultraviolet cross sections of ozone, I. The measurements. in: CS Zerefos and A Ghazi (Eds.), Proceedings of the Quadriennal Ozone Symp., Halkidiki, 1985, Greece, p. 606, D. Reidel, Hingham, MA.

Godin S., G. Mégie, J. Pelon : Systematic Lidar Measurements of the Stratospheric Ozone vertical Distribution, Geophys. Res. Letters, Vol 16 No 16, 547-550, 1989.

Godin S., A. Carswell, D. Donovan, H. Claude, W. Steinbrecht,S. Mcdermid, T. Mcgee, M.R. Gross, H. Nakane, D.P.J. Swart, J.B. Bergwerff, O. Uchino, P. Von Der Gathen, R. Neuber, Ozone Differential Absorption Lidar Algorithm Intercomparison, Appl. Opt., Vol 38, 30, 6225-6236, 1999

Godin-Beekmann, S., J. Porteneuve, A. Garnier, Systematic DIAL ozone measurements at Observatoire de Haute-Provence, J. Env. Monitoring, 5, 57-67, 2003

Nair, P. J., Godin-Beekmann, S., Froidevaux, L., Flynn, L. E., Zawodny, J. M., Russell III, J. M., Pazmi˜no, A., Ancellet, G., Steinbrecht, W., Claude, H., Leblanc, T., McDermid, S., van Gijsel, J. A. E., Johnson, B., Thomas, A., Hubert, D., Lambert, J.-C., Nakane, H., and Swart, D. P. J.: Relative drifts and stability of satellite and ground-based stratospheric ozone profiles at NDACC lidar stations, Atmos. Meas. Tech., 5, 1301–1318, doi:10.5194/amt-5-1301-2012, 2012. 7085, 7091

S. Godin, G. Mégie and J. Pelon, Geophys. Res. Lett., 1989, 16(16), 547–550. H. Nakane, N. Sugimoto, S. Hayashida, Y. Sasano and I. Matsui, Five years lidar observation of vertical profiles of stratospheric ozone at NIES, Tsukuba (36N, 140E), Proc. 17th ILRC, Sendai, Japan, 1994.

T. J. McGee, M. Gross, R. Ferrare, W. S. Heaps and U. N. Singh, Geophys. Res. Lett., 1993, 20, 955–958.